Latin American Journal of Solids and Structures
www.lajss.org

Size-dependent vibrations of post-buckled functionally graded Mindlin rectangular microplates

Abstract

In this paper, the free vibration behavior of post-buckled functionally graded (FG) Mindlin rectangular microplates are described based on the modified couple stress theory (MCST). This theory enables the consideration of the size-effect through introducing material length scale parameters. The FG microplates made of a mixture of metal and ceramic are considered whose volume fraction of components is expressed by a power law function. By means of Hamilton's principle, the nonlinear governing equations and associated boundary conditions are derived for FG microplates in the postbuckling domain. The governing equations and boundary conditions are then discretized by using the generalized differential quadrature (GDQ) method before solving numerically by the pseudo-arclength continuation technique. In the solution procedure, the postbuckling problem of microplates is investigated first. Afterwards, the free vibration of microplates around the buckled configuration is discussed. The effects of dimensionless length scale parameter, material gradient index and aspect ratio on the on the postbuckling path and frequency of FG microplates subject to arbitrary edge supports are thoroughly discussed.

Keywords

Mindlin plate theory; Small scale effect; Modified couple stress theory; Free vibration; Post-buckled FG rectangular microplate; Generalized differential quadrature.

R. Ansari *
M. FaghihShojaei
V. Mohammadi
R. Gholami, M. A. Darabi

Department of Mechanical Engineering
University of Guilan, Rasht, Iran, P.O. Box 41635-3756

* Corresponding author
Tel. /fax: +98 131 6690276.
E-mail address: r_ansari@guilan.ac.ir

Received 24.10.2013
In revised form 23.05.2014
Accepted 28.05.2014
Available online 10.09.2014

1 INTRODUCTION

Functionally graded (FG) materials are increasingly being used in microstructures because of their potentiality in acquiring desired performance. Hence, many researchers have intensified their efforts to employ them in micro-electromechanical systems (MEMS) and atomic force microscopes (Lü et al. 2009a; Lü et al. 2009b; Mahmud et al. 2008; Hasanyan et al. 2008; Witvrouw et al. 2005).

Of all the basic microstructures, microbeams and microplates are broadly used in MEMS. There are several micro-torsion and micro-bending experiments which have reported the size-dependent deformation behavior in microbeams. Hence, considering the size effect is essential in the study of FG micro- and nano- structures. Since the conventional continuum mechanics theory is incapable of considering the size effect in micro and nano structures, different attempts have been made to develop several successful size-dependent theories (Mindlin and Tiersten 1962; Eringen 1972; Lam et al. 2003). These theories and their modified forms have been efficiently used in different studies (Wang 2010; Ansari et al. 2011; Claeyssen et al. 2013; Ansari et al. 2012; Chang 2013; Ramezani 2012; Wang and Feng 2007; Ghayesh et al. 2013; Farokhi et al. 2013).

The classical couple stress theory established by Mindlin and Tiersten (1962) and Toupin (1962) comprises two classical and two additional material constants for isotropic elastic materials. The modified form of this theory (MCST) was proposed by Yang et al. (2002); they considered only one additional material length scale parameter besides two classical material constants and facilitated incorporating the size effect. This theory has been employed to develop several size-dependent microbeams and microplates. In this direction, the static and dynamic behavior of size-dependent Kirchhoff microplates is investigated analytically in several papers (Tsiatas 2009; Yin et al. 2010; Jomehzadeh et al. 2011). In another study, free vibration behavior of Mindlin microplates is examined based on the MCST (Ke et al. 2012a). The free vibration of FG microbeams is studied by Asghari et al. (2010) in the context of the Bernoulli–Euler beam theory. Also, in another work, they examined the static bending and free vibration of cantilever and simply-supported FG microbeams based on the MCST (Asghari et al. 2011). The dynamic stability of FG microbeams is also studied by Ke and Wang (2011) based on the MCST and the Timoshenko beam theories. Based on the MCST, the nonlinear free vibration of size-dependent FG microbeams is investigated by Ke et al. (2011). Ke et al. (2012b) studied the bending, buckling and free vibration of annular FG microplates based on the MCST and Mindlin plate theory.

Microplates are usually subjected to forces which can cause buckling and postbuckling. In this paper, the free vibration behavior of post-buckled FG Mindlin rectangular microplates is investigated. To this end, firstly, the MCST and Hamilton's principle are used to obtain the nonlinear governing equations and associated boundary conditions of FG microplates in the postbuckling configuration. Then, the GDQ method and the pseudo-arclength continuation technique are employed to discretize and solve the governing equations and boundary conditions.

2 GOVERNING EQUATIONS OF SIZE-DEPENDET FG MINDLIN RECTANGULAT MICROPLATES

Based on the MCST (Yang et al. 2002), the strain energy of a continuum elastic medium taking up region Ω can be expressed by a function of strain tensor and gradient of the rotation vector as

$$U_m = \frac{1}{2}\int_{\Omega}\left(\boldsymbol{\sigma} : \boldsymbol{\varepsilon} + \mathbf{m} : \boldsymbol{\chi}\right)dv \tag{1}$$

where $\boldsymbol{\sigma}$ is the Cauchy stress tensor; $\boldsymbol{\varepsilon}$ denotes the infinitesimal strain tensor; $\boldsymbol{\chi}^s$ is the symmetric rotation gradient tensor and $\mathbf{m}$ stands for the deviatoric part of the couple stress tensor defined for a linear isotropic elastic material. Following are the definitions of mentioned tensors (Timoshenko and Goodier 1970; Kovalenko 1969; Ke et al. 2010)

$$\boldsymbol{\varepsilon}=\frac{1}{2}\left(\nabla\mathbf{u}+\left(\nabla\mathbf{u}\right)^{\mathrm{T}}+\left(\nabla\mathbf{u}\right)\left(\nabla\mathbf{u}\right)^{\mathrm{T}}\right);\ \varepsilon_{ij}=\frac{1}{2}\left(u_{i,j}+u_{j,i}+u_{i,j}u_{j,i}\right), \tag{2a}$$

$$\boldsymbol{\chi}^{s}=\frac{1}{2}\left(\nabla\boldsymbol{\theta}+\left(\nabla\boldsymbol{\theta}\right)^{\mathrm{T}}\right);\ \chi_{\mathrm{ij}}^{\mathrm{s}}=\frac{1}{2}\left(\theta_{\mathrm{i,j}}+\theta_{\mathrm{j,i}}\right),\ \ \theta_{i}=\frac{1}{2}\left(\mathrm{curl}\left(\mathbf{u}\right)\right)_{\mathrm{i}}, \tag{2b}$$

$$\boldsymbol{\sigma}=\lambda tr\left(\boldsymbol{\varepsilon}\right)\mathbf{I}+2\mu\boldsymbol{\varepsilon},\ \ \mathbf{m}=2\mu l^{2}\boldsymbol{\chi}^{s}. \tag{2c}$$

in which $\mathbf{u}$ is the displacement vector and $\boldsymbol{\theta}$ is the rotation vector. Lame's constants are denoted by $\lambda=E\nu/\left(\left(1+\nu\right)\left(1-2\nu\right)\right)$ and $\mu=E/2\left(1+\nu\right)$; where ν and E are Poisson's ratio and Young's modulus, respectively. l represents a material length scale parameter whose value can be specified via micro-torsion tests of slim cylinders or micro-bending tests of thin beams.

A schematic of an FG microplate with the length a, width b and thickness h made of a mixture of ceramics and metals is illustrated in figure 1.

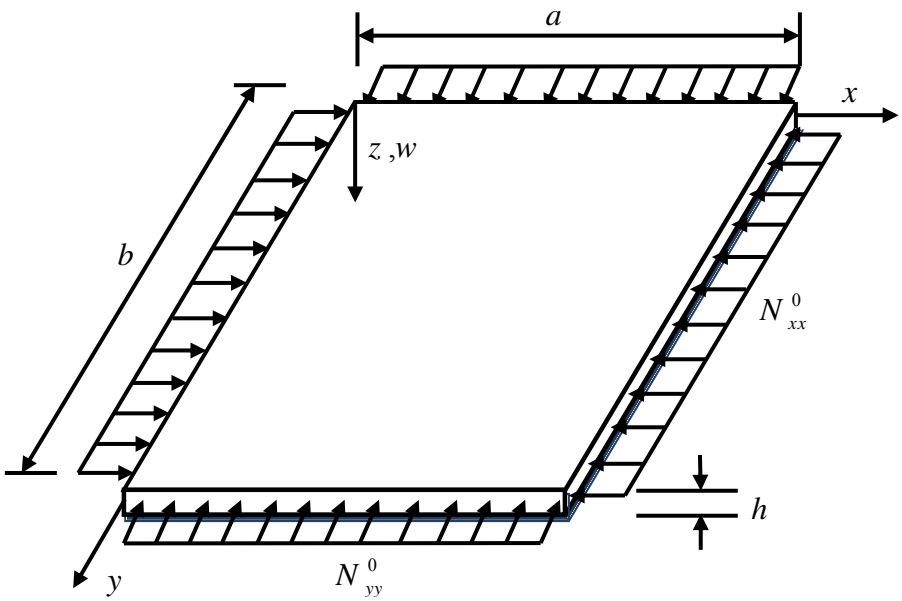

Figure 1: Schematic of a microplate: kinematic parameters, coordinate system, geometry and loading

The materials of the FG microplate at bottom surface $\left(\mathrm{z}=-\mathrm{h}/2\right)$ and top surface $\left(\mathrm{z}=\mathrm{h}/2\right)$ are supposed to be metal-rich and ceramic-rich, respectively. The effective material properties of the FG microplate, namely Young's modulus, Poisson's ratio and mass density can be approximated by

$$\mathrm{E}\left(\mathrm{z}\right)=\mathrm{E}_{\mathrm{c}}\mathrm{V}_{\mathrm{c}}+\mathrm{E}_{\mathrm{m}}\mathrm{V}_{\mathrm{m}},\ \ \nu\left(\mathrm{z}\right)=\nu_{\mathrm{c}}\mathrm{V}_{\mathrm{c}}+\nu_{\mathrm{m}}\mathrm{V}_{\mathrm{m}},\ \ \rho\left(\mathrm{z}\right)=\rho_{\mathrm{c}}\mathrm{V}_{\mathrm{c}}+\rho_{\mathrm{m}}\mathrm{V}_{\mathrm{m}}. \tag{3}$$

in which V denotes the volume fraction of the phase materials; the subscripts m and c symbolize metal and ceramic phases, respectively. To express the volume fraction of FG microplate's components, the power law function is used as (Fares et al. 2009)

$$V_c(z)=\left(\frac{1}{2}+\frac{z}{h}\right)^n \quad , \quad V_m(z)=1-\left(\frac{1}{2}+\frac{z}{h}\right)^n \tag{4}$$

in which n denotes the volume fraction exponent.

Based on the first-order shear deformation plate theory, the in-plane displacements can be stated as linear functions of the plate thickness and the transverse displacement is considered to be unchanged through the plate thickness; considering these assumptions, the displacement field in a Mindlin plate can be described as

$$u_x=u(t,x,y)-z\psi_x(t,x,y),\quad u_y=v(t,x,y)-z\psi_y(t,x,y),\quad u_z=w(t,x,y). \tag{5}$$

in which t is the time, x, y, z denote the coordinates of Cartesian coordinate system and $u(t,x,y)$ and $v(t,x,y)$ are mid-plane displacements, and $w(t,x,y)$ represents the lateral deflection of the microplate. Using Eq. (5) and Eq. (2a) leads to the nonzero components of the strain-displacement equations as follows

$$\varepsilon_{xx}=\phi_0-z\phi_1,\ \varepsilon_{yy}=\varphi_0-z\varphi_1,\ \varepsilon_{xy}=\varepsilon_{yx}=(\kappa_0-z\kappa_1)/2,\varepsilon_{xz}=\varepsilon_{zx}=\gamma_1/2,\ \varepsilon_{yz}=\varepsilon_{zy}=\gamma_2/2. \tag{6}$$

where

$$\begin{aligned}&\phi_0=u_{,x}+\frac{1}{2}w_{,x}^2,\ \phi_1=\psi_{x,x},\ \varphi_0=v_{,y}+\frac{1}{2}w_{,y}^2,\varphi_1=\psi_{y,y},\\&\kappa_0=u_{,y}+v_{,x}+w_{,x}w_{,y},\quad \kappa_1=\psi_{x,y}+\psi_{y,x},\ \gamma_1=w_{,x}-\psi_x,\ \gamma_2=w_{,y}-\psi_y.\end{aligned} \tag{7}$$

in which comma denotes partial differentiation with respect to the coordinates.

By inserting Eq. (5) into Eq.(2b), the rotations of material elements within the microplate are introduced as

$$\theta_x=\frac{1}{2}(w_{,y}+\psi_y),\quad \theta_y=-\frac{1}{2}(w_{,x}+\psi_x),\ \theta_z=\frac{1}{2}(v_{,x}-u_{,y})-\frac{z}{2}(\psi_{y,x}-\psi_{x,y}). \tag{8}$$

Also, by substituting θ_x,θ_y and θ_z into Eq. (2b) the components of symmetric rotation gradient tensor are expressed by

$$\begin{aligned}&\chi^s_{xx}=\frac{1}{2}(w_{,xy}+\psi_{y,x}),\ \chi^s_{yy}=-\frac{1}{2}(w_{,xy}+\psi_{x,y}),\ \chi^s_{zz}=\frac{1}{2}(\psi_{x,y}-\psi_{y,x}),\\&\chi^s_{xy}=\frac{1}{4}(w_{,yy}-w_{,xx}+\psi_{y,y}-\psi_{x,x}),\ \chi^s_{xz}=\frac{1}{4}(v_{,xx}-u_{,xy})+\frac{z}{4}(\psi_{x,xy}-\psi_{y,xx}),\\&\chi^s_{yz}=\frac{1}{4}(v_{,xy}-u_{,yy})+\frac{z}{4}(\psi_{x,yy}-\psi_{y,xy}).\end{aligned} \tag{9}$$

By inserting the classical strain and symmetric rotation gradient tensors according to Eqs. (6) and (9) into Eq. (2c), the classical stress tensor $\boldsymbol{\sigma}$ and the couple stresses $\mathbf{m}^s$ are achieved.

By considering Π_{C} as the strain energy related to the classical theory and Π_{NC} as the strain energy related to the modified couple stress theory, respectively, the total strain energy of FG microplates can be written as $\Pi_{\mathrm{s}} = \Pi_{\mathrm{C}} + \Pi_{\mathrm{NC}}$, where

$$\begin{aligned}\Pi_C = \frac{1}{2}\int_A \Big\{ & N_{xx}\left(u_{,x} + \frac{1}{2}w_{,x}^{2}\right) - M_{xx}\psi_{\mathrm{x,x}} + N_{yy}\left(v_{,y} + \frac{1}{2}w_{,y}^{2}\right) - M_{yy}\psi_{\mathrm{y,y}} \\ & + N_{xy}\left(u_{,y} + \mathrm{v}_{,\mathrm{x}} + \mathrm{w}_{,\mathrm{x}}w_{,y}\right) - M_{xy}\left(\psi_{\mathrm{x,y}} + \psi_{\mathrm{y,x}}\right) + Q_x\left(\mathrm{w}_{,\mathrm{x}} - \psi_{\mathrm{x}}\right) + Q_y\left(\mathrm{w}_{,\mathrm{y}} - \psi_{\mathrm{y}}\right)\Big\} dA\end{aligned} \tag{10a}$$

$$\begin{aligned}\Pi_{NC} = \frac{1}{2}\int_A \Big\{ & \frac{Y_{xx}}{2}\left(w_{,xy} + \psi_{\mathrm{y,x}}\right) - \frac{Y_{yy}}{2}\left(w_{,xy} + \psi_{\mathrm{x,y}}\right) + \frac{Y_{zz}}{2}\left(\psi_{\mathrm{x,y}} - \psi_{\mathrm{y,x}}\right) \\ & + \frac{Y_{xy}}{2}\left(w_{,yy} - \mathrm{w}_{,\mathrm{xx}} + \psi_{\mathrm{y,y}} - \psi_{\mathrm{x,x}}\right) + \frac{Y_{xz}}{2}\left(v_{,xx} - \mathrm{u}_{,\mathrm{xy}}\right) + \frac{Y_{yz}}{2}\left(v_{,xy} - \mathrm{u}_{,\mathrm{yy}}\right) \\ & + \frac{H_{xz}}{2}\left(\psi_{\mathrm{x,xy}} - \psi_{\mathrm{y,xx}}\right) + \frac{H_{yz}}{2}\left(\psi_{\mathrm{x,yy}} - \psi_{\mathrm{y,xy}}\right)\Big\} dA\end{aligned} \tag{10b}$$

in which the in-plane force resultants $\left(\mathrm{N}_{\mathrm{xx}}, \mathrm{N}_{\mathrm{yy}}, \mathrm{N}_{\mathrm{xy}}\right)$, moment resultants $\left(\mathrm{M}_{\mathrm{xx}}, \mathrm{M}_{\mathrm{yy}}, \mathrm{M}_{\mathrm{xy}}\right)$, transverse force resultants $\left(\mathrm{Q}_{\mathrm{x}}, \mathrm{Q}_{\mathrm{y}}\right)$, couple moments $\left(\mathrm{Y}_{\mathrm{xx}}, \mathrm{Y}_{\mathrm{yy}}, \mathrm{Y}_{\mathrm{zz}}, \mathrm{Y}_{\mathrm{xy}}, \mathrm{Y}_{\mathrm{xz}}, \mathrm{Y}_{\mathrm{yz}}\right)$ and higher-order couple moments $\left(\mathrm{H}_{\mathrm{xz}}, \mathrm{H}_{\mathrm{yz}}\right)$ are obtained as

$$\mathbf{N} = \begin{Bmatrix} N_{xx} \\ N_{yy} \\ N_{xy} \end{Bmatrix} = \int_{-h/2}^{h/2} \begin{Bmatrix} \sigma_{xx} \\ \sigma_{yy} \\ \sigma_{xy} \end{Bmatrix} dz \,, \mathbf{M} = \begin{Bmatrix} M_{xx} \\ M_{yy} \\ M_{xy} \end{Bmatrix} = \int_{-h/2}^{h/2} \begin{Bmatrix} \sigma_{xx} \\ \sigma_{yy} \\ \sigma_{xy} \end{Bmatrix} z dz \,, \mathbf{Q} = \begin{Bmatrix} Q_x \\ Q_y \end{Bmatrix} = K_S \int_{-h/2}^{h/2} \begin{Bmatrix} \sigma_{xz} \\ \sigma_{yz} \end{Bmatrix} dz \,, \tag{11a}$$

$$\begin{aligned}\mathbf{Y} &= \left\{Y_{xx}, Y_{yy}, Y_{zz}, Y_{xy}, Y_{xz}, Y_{yz}\right\} = \int_{-h/2}^{h/2} \left\{m_{xx}^{s}, m_{yy}^{s}, m_{zz}^{s}, m_{xy}^{s}, m_{xz}^{s}, m_{yz}^{s}\right\} dz \,, \\ \mathbf{H} &= \left\{H_{xz}, H_{yz}\right\} = \int_{-h/2}^{h/2} \left\{m_{xz}^{s}, m_{yz}^{s}\right\} z dz \,,\end{aligned} \tag{11b}$$

in which the parameter K_S denotes the shear correction factor.

Now, by defining the following parameters

$$\begin{aligned}\left\{\mathrm{A}_{11}, \mathrm{B}_{11}, \mathrm{D}_{11}\right\} &= \int_{-\mathrm{h}/2}^{\mathrm{h}/2} \frac{E\left(1-\nu\right)}{\left(1+\nu\right)\left(1-2\nu\right)} \left\{1, \mathrm{z}, \mathrm{z}^2\right\} \mathrm{dz}, \\ \left\{\mathrm{A}_{12}, \mathrm{B}_{12}, \mathrm{D}_{12}\right\} &= \int_{-\mathrm{h}/2}^{\mathrm{h}/2} \frac{E\nu}{\left(1+\nu\right)\left(1-2\nu\right)} \left\{1, \mathrm{z}, \mathrm{z}^2\right\} \mathrm{dz}, \\ \left\{\mathrm{A}_{55}, \mathrm{B}_{55}, \mathrm{D}_{55}\right\} &= \int_{-\mathrm{h}/2}^{\mathrm{h}/2} \frac{E}{2\left(1+\nu\right)} \left\{1, \mathrm{z}, \mathrm{z}^2\right\} \mathrm{dz},\end{aligned} \tag{12}$$

the force resultants and moment resultants based on Eq. (11) can be written in terms of displacements as following

$$\begin{aligned}
N_{xx} &= A_{11}\left(u_{,x}+\frac{1}{2}w_{,x}^{2}\right)+A_{12}\left(v_{,y}+\frac{1}{2}w_{,y}^{2}\right)-B_{11}\psi_{x,x}-B_{12}\psi_{y,y},\\
N_{yy} &= A_{11}\left(v_{,y}+\frac{1}{2}w_{,y}^{2}\right)+A_{12}\left(u_{,x}+\frac{1}{2}w_{,x}^{2}\right)-B_{11}\psi_{y,y}-B_{12}\psi_{x,x},\\
N_{xy} &= A_{55}\left(u_{,y}+v_{,x}+w_{,x}w_{,y}\right)-B_{55}\left(\psi_{x,y}+\psi_{y,x}\right),
\end{aligned} \tag{13a}$$

$$\begin{aligned}
M_{xx} &= B_{11}\left(u_{,x}+\frac{1}{2}w_{,x}^{2}\right)+B_{12}\left(v_{,y}+\frac{1}{2}w_{,y}^{2}\right)-D_{11}\psi_{x,x}-D_{12}\psi_{y,y},\\
M_{yy} &= B_{11}\left(v_{,y}+\frac{1}{2}w_{,y}^{2}\right)+B_{12}\left(u_{,x}+\frac{1}{2}w_{,x}^{2}\right)-D_{11}\psi_{y,y}-D_{12}\psi_{x,x},\\
M_{xy} &= B_{55}\left(u_{,y}+v_{,x}+w_{,x}w_{,y}\right)-D_{55}\left(\psi_{x,y}+\psi_{y,x}\right),
\end{aligned} \tag{13b}$$

$$Q_x = \kappa_s A_{55}\left(w_{,x}-\psi_x\right),\ Q_y = \kappa_s A_{55}\left(w_{,y}-\psi_y\right), \tag{13c}$$

$$\begin{aligned}
&Y_{xx} = A_{55}l^2\left(w_{,xy}+\psi_{y,x}\right),\ Y_{yy} = -A_{55}l^2\left(w_{,xy}+\psi_{x,y}\right),\\
&Y_{zz} = A_{55}l^2\left(\psi_{x,y}-\psi_{y,x}\right), Y_{xy} = \frac{A_{55}l^2}{2}\left(w_{,yy}-w_{,xx}+\psi_{y,y}-\psi_{x,x}\right),\\
&Y_{xz} = \frac{A_{55}l^2}{2}\left(v_{,xx}-u_{,xy}\right)+\frac{B_{55}l^2}{2}\left(\psi_{x,xy}-\psi_{y,xx}\right),\\
&Y_{yz} = \frac{A_{55}l^2}{2}\left(v_{,xy}-u_{,yy}\right)+\frac{B_{55}l^2}{2}\left(\psi_{x,yy}-\psi_{y,xy}\right).
\end{aligned} \tag{13d}$$

$$\begin{aligned}
H_{xz} &= \frac{B_{55}l^2}{2}\left(v_{,xx}-u_{,xy}\right)+\frac{D_{55}l^2}{2}\left(\psi_{x,xy}-\psi_{y,xx}\right),\\
H_{yz} &= \frac{B_{55}l^2}{2}\left(v_{,xy}-u_{,yy}\right)+\frac{D_{55}l^2}{2}\left(\psi_{x,yy}-\psi_{y,xy}\right).
\end{aligned} \tag{13e}$$

The work Π_w due to the in-plane forces N_{xx}^0, N_{yy}^0 and N_{xy}^0 can be achieved as

$$\Pi_w = \frac{1}{2}\int_A\left(N_{xx}^0 w_{,x}^2+2N_{xy}^0 w_{,x}w_{,y}+N_{yy}^0 w_{,y}^2\right)dA, \tag{14}$$

Also, for the kinematic energy one can write the following relation

$$\begin{aligned}
\Pi_T &= \frac{1}{2}\int_{A}\int_{-h/2}^{h/2}\left\{\left(\dot{u}-z\dot{\psi}_x\right)^2+\left(\dot{v}-z\dot{\psi}_y\right)^2+\dot{w}^2\right\}dz dA\\
&= \int_A\left\{I_0\left(\dot{u}^2+\dot{v}^2+\dot{w}^2\right)-2I_1\left(\dot{u}\dot{\psi}_x+\dot{v}\dot{\psi}_y\right)+I_2\left(\dot{\psi}_x^2+\dot{\psi}_y^2\right)\right\}dA
\end{aligned} \tag{15}$$

in which the overdot symbolizes differentiation with respect to time; ρ and A are the density and area occupied by the mid-plane of the microplate, respectively and

$$\{I_0, I_1, I_2\} = \int_{-h/2}^{h/2} \rho(z)\{1, z, z^2\}\, dz. \tag{16}$$

In the following, Hamilton's principle is employed to derive the governing equations of motion and corresponding boundary conditions. Hamilton's principle can be mathematically defined as

$$\delta \int_{t_1}^{t_2} (\Pi_T - \Pi_s + \Pi_w) dt = 0, \tag{17}$$

To this end, first by taking the variation of u, v, w, ψ_x and ψ_y, then by performing integration by parts, and finally, by setting the coefficients of $\delta u, \delta v, \delta w, \delta\psi_x$ and $\delta\psi_y$ equal to zero, one can achieve to the following expressions for the governing equations of motion and the boundary conditions

$$N_{xx,x} + N_{xy,y} + \frac{1}{2}(Y_{xz,xy} + Y_{yz,yy}) = I_0\ddot{u} - I_1\ddot{\psi}_x, \tag{18a}$$

$$N_{xy,x} + N_{yy,y} - \frac{1}{2}(Y_{xz,xx} + Y_{yz,xy}) = I_0\ddot{v} - I_1\ddot{\psi}_y, \tag{18b}$$

$$\begin{aligned} &Q_{x,x} + Q_{y,y} + \frac{1}{2}Y_{xy,xx} + \frac{1}{4}(Y_{yy,xy} - Y_{xx,xy}) - \frac{1}{2}Y_{xy,yy} + (N_{xx}w_{,x})_{,x} + (N_{yy}w_{,y})_{,y} \\ &+ (N_{xy}w_{,y})_{,x} + (N_{xy}w_{,x})_{,y} + N^0_{xx}w_{,xx} + N^0_{yy}w_{,yy} + 2N^0_{xy}w_{,xy} = I_0\ddot{w}, \end{aligned} \tag{18c}$$

$$M_{xx,x} + M_{xy,y} - Q_x + \frac{1}{2}(Y_{yy,y} + Y_{xy,x} - Y_{zz,y} + H_{xz,xy} + H_{yz,yy}) = I_2\ddot{\psi}_x - I_1\ddot{u}, \tag{18d}$$

$$M_{xy,x} + M_{yy,y} - Q_y + \frac{1}{2}(Y_{zz,x} - Y_{xx,x} - Y_{xy,y} - H_{xz,xx} - H_{yz,xy}) = I_2\ddot{\psi}_y - I_1\ddot{v}, \tag{18e}$$

$$\begin{aligned} &\delta u = 0 \quad or \quad \left(N_{xx} + \frac{1}{4}Y_{xz,y}\right)n_x + \left(N_{xy} + \frac{1}{4}Y_{xz,x} + \frac{1}{2}Y_{yz,y}\right)n_y = 0, \\ &\delta u_{,x} = 0 \quad or \quad \left(\frac{Y_{xz}}{4}\right)n_y = 0, \quad \delta u_{,y} = 0 \quad or \quad \left(\frac{Y_{xz}}{4}\right)n_x + \left(\frac{Y_{yz}}{2}\right)n_y = 0, \end{aligned} \tag{18f}$$

$$\begin{aligned} &\delta v = 0 \quad or \quad \left(N_{xy} - \frac{1}{2}Y_{xz,x} - \frac{1}{4}Y_{yz,y}\right)n_x + \left(N_{yy} - \frac{1}{4}Y_{yz,x}\right)n_y = 0, \\ &\delta v_{,x} = 0 \quad or \quad \left(\frac{Y_{xz}}{2}\right)n_x + \left(\frac{Y_{yz}}{4}\right)n_y = 0, \quad \delta v_{,y} = 0 \quad or \quad \left(\frac{Y_{yz}}{4}\right)n_x = 0, \end{aligned} \tag{18g}$$

$$\delta w = 0 \; or \left(Q_x + \frac{1}{2} Y_{xy,x} + \frac{1}{4}\left(Y_{yy,y} - Y_{xx,y}\right) + \left(N_{xx} + N^0_{xx}\right) w_{,x} + \left(N_{xy} + N^0_{xy}\right) w_{,y} \right) n_x$$
$$+ \left(Q_y - \frac{1}{2} Y_{xy,y} + \frac{1}{4}\left(Y_{yy,x} - Y_{xx,x}\right) + \left(N_{yy} + N^0_{yy}\right) w_{,y} + \left(N_{xy} + N^0_{xy}\right) w_{,x} \right) n_y = 0, \tag{18h}$$
$$\delta w_{,x} = 0 \;\; or \;\; \left(\frac{1}{2} Y_{xy}\right) n_x + \left(\frac{Y_{yy} - Y_{xx}}{4}\right) n_y = 0,$$

$$\delta w_{,y} = 0 \;\; or \;\; \left(\frac{Y_{yy} - Y_{xx}}{4}\right) n_x + \left(\frac{1}{2} Y_{xy}\right) n_y = 0.$$

$$\delta \psi_x = 0 \; or \left(M_{xx} + \frac{Y_{xy}}{2} + \frac{1}{4} H_{xz,y} \right) n_x + \left(M_{xy} + \frac{Y_{yy} - Y_{zz}}{2} + \frac{1}{2} H_{yz,y} + \frac{1}{4} H_{xz,x} \right) n_y = 0, \tag{18i}$$
$$\delta \psi_{x,x} = 0 \; or \; \left(\frac{1}{4} H_{xz}\right) n_y = 0, \;\; \delta \psi_{x,y} = 0 \;\; or \;\; \left(\frac{1}{4} H_{xz}\right) n_x + \left(\frac{1}{2} H_{yz}\right) n_y = 0.$$

$$\delta \psi_y = 0 \; or \left(M_{xy} + \frac{Y_{zz} - Y_{xx}}{2} - \frac{1}{2} H_{xz,x} - \frac{1}{4} H_{yz,y} \right) n_x + \left(M_{yy} - \frac{1}{2} Y_{xy} - \frac{1}{4} H_{yz,x} \right) n_y = 0,$$
$$\delta \psi_{y,x} = 0 \; or \left(\frac{1}{2} H_{xz}\right) n_x + \left(\frac{1}{4} H_{yz}\right) n_y = 0, \; \delta \psi_{y,y} = 0 \;\; or \;\; \left(\frac{1}{4} H_{yz}\right) n_x = 0. \tag{18j}$$

Eqs. (18f)–(18j) provide different possible boundary conditions for the size-dependent FG rectangular microplate. For example, the boundary conditions related to FG microplates with all clamped edges (CCCC) are as

$$\begin{aligned} &u = v = w = \psi_x = \psi_y = v_{,x} = w_{,x} = \psi_{y,x} = 0; \;\; \text{at edges } x = 0, a. \\ &u = v = w = \psi_x = \psi_y = u_{,y} = w_{,y} = \psi_{x,y} = 0; \;\; \text{at edges } y = 0, b. \end{aligned} \tag{19}$$

and for FG microplates with fully simply supported edges (SSSS):

$$\begin{aligned} &u = v = w = M_{xx} + \frac{1}{2} Y_{xy} + \frac{1}{4} H_{xz,y} = 0, \\ &M_{xy} + \frac{Y_{zz} - Y_{xx}}{2} - \frac{1}{2} H_{xz,x} - \frac{1}{4} H_{yz,y} = Y_{xz} = Y_{xy} = H_{xz} = 0; \;\; \text{at edges } x = 0, a. \end{aligned} \tag{20a}$$

$$\begin{aligned} &u = v = w = M_{xy} + \frac{Y_{yy} - Y_{zz}}{2} + \frac{1}{2} H_{yz,y} + \frac{1}{4} H_{xz,x} = 0, \\ &M_{yy} - \frac{1}{2} Y_{xy} - \frac{1}{4} H_{yz,x} = Y_{yz} = Y_{xy} = H_{yz} = 0; \;\; \text{at edges } y = 0, b. \end{aligned} \tag{20b}$$

By introducing the following non-dimensional parameters

$$
\begin{aligned}
&x=\frac{x}{a}, y=\frac{y}{b},\quad (u,v,w)\to(hu,hv,hw),(\eta_1,\eta_2)=\left(\frac{a}{h},\frac{b}{h}\right),\ \kappa=\frac{a}{b},\tau=\frac{t}{a}\sqrt{\frac{A_{110}}{I_{00}}},\\
&(a_{11},a_{12},a_{55})=\left(\frac{A_{11}}{A_{110}},\frac{A_{33}}{A_{110}},\frac{A_{55}}{A_{110}}\right),(b_{11},b_{12},b_{55})=\left(\frac{B_{11}}{A_{110}h},\frac{B_{12}}{A_{110}h},\frac{B_{55}}{A_{110}h}\right),\\
&(d_{11},d_{12},d_{55})=\left(\frac{D_{11}}{A_{110}h^2},\frac{D_{12}}{A_{110}h^2},\frac{D_{55}}{A_{110}h^2}\right),(\bar{I}_0,\bar{I}_1,\bar{I}_2)=\left(\frac{I_0}{I_{00}},\frac{I_1}{I_{00}h},\frac{I_2}{I_{00}h^2}\right),\\
&\ell=\frac{l}{h}\ ,\ \bar{N}^0_{xx}=\frac{N^0_{xx}}{A_{110}},\bar{N}^0_{xy}=\frac{N^0_{xy}}{A_{110}},\bar{N}^0_{yy}=\frac{N^0_{yy}}{A_{110}},\beta=\frac{\ell^2}{4\eta_1^2}.
\end{aligned}
\tag{21}
$$

where A_{110} and I_{00} are the values A_{11} and I_0 of a homogeneous metal microplate,One can express the nonlinear governing equations as follows

$$
\begin{aligned}
&a_{11}u_{,xx}+\kappa^2a_{55}u_{,yy}+\kappa(a_{12}+a_{55})v_{,xy}-b_{11}\psi_{x,xx}-\kappa^2b_{55}\psi_{x,yy}-\kappa(b_{12}+b_{55})\psi_{y,xy}\\
&-\beta\left(\kappa^4\left(a_{55}u_{,yyyy}-b_{55}\psi_{x,yyyy}\right)+\kappa^2\left(a_{55}u_{,xxyy}-b_{55}\psi_{x,xxyy}\right)-\kappa\left(a_{55}v_{,xxxy}-b_{55}\psi_{y,xxxy}\right)\right)\\
&+\beta\kappa^3\left(a_{55}v_{,xyyy}-b_{55}\psi_{y,xyyy}\right)+Z_1=\bar{I}_0\ddot{u}-\bar{I}_1\ddot{\psi}_x,
\end{aligned}
\tag{22a}
$$

$$
\begin{aligned}
&\kappa(a_{12}+a_{55})u_{,xy}+\kappa^2a_{11}v_{,yy}+a_{55}v_{,xx}-\kappa(b_{12}+b_{55})\psi_{x,xy}-\kappa^2b_{11}\psi_{y,yy}-b_{55}\psi_{y,xx}\\
&-\beta\left(\left(a_{55}v_{,xxxx}-b_{55}\psi_{y,xxxx}\right)+\kappa^2\left(a_{55}v_{,xxyy}-b_{55}\psi_{y,xxyy}\right)-\kappa\left(a_{55}u_{,xxxy}-b_{55}\psi_{x,xxxy}\right)\right)\\
&+\beta\kappa^3\left(a_{55}u_{,xyyy}-b_{55}\psi_{x,xyyy}\right)+Z_2=\bar{I}_0\ddot{v}-\bar{I}_1\ddot{\psi}_y,
\end{aligned}
\tag{22b}
$$

$$
\begin{aligned}
&k_sa_{55}\left(w_{,xx}+\kappa^2w_{,yy}-\eta_1\psi_{x,x}-\eta_1\kappa\psi_{y,y}\right)-a_{55}\beta\left(w_{,xxxx}+2\kappa^2w_{,xxyy}+\kappa^4w_{,yyyy}\right)\\
&-a_{55}\beta\eta_1\left(\psi_{x,xxx}+\kappa^2\psi_{x,xyy}+\kappa\psi_{y,xxy}+\kappa^3\psi_{y,yyy}\right)\\
&+\bar{N}^0_{xx}w_{,xx}+2N^0_{xy}\kappa w_{,xy}+N^0_{yy}\kappa^2w_{,yy}+Z_3=\bar{I}_0\ddot{w},
\end{aligned}
\tag{22c}
$$

$$
\begin{aligned}
&-b_{11}u_{,xx}-b_{55}\kappa^2u_{,yy}-\kappa(b_{12}+b_{55})v_{,xy}+d_{11}\psi_{x,xx}+\kappa^2d_{55}\psi_{x,yy}+\kappa(d_{55}+d_{12})\psi_{y,xy}\\
&+\beta\left(-\kappa\left(b_{55}v_{,xxxy}-d_{55}\psi_{y,xxxy}\right)-\kappa^3\left(b_{55}v_{,xyyy}-d_{55}\psi_{y,xyyy}\right)+\kappa^2\left(b_{55}u_{,xxyy}-d_{55}\psi_{x,xxyy}\right)\right)\\
&+\beta\left(\kappa^4\left(b_{55}u_{,yyyy}-d_{55}\psi_{x,yyyy}\right)+a_{55}\eta_1\left(w_{,xxx}+\kappa^2w_{,xyy}\right)\right)\\
&+a_{55}\ell^2\left(\frac{1}{4}\psi_{x,xx}+\kappa^2\psi_{x,yy}-\frac{3\kappa}{4}\psi_{y,xy}\right)+K_Sa_{55}\eta_1\left(w_{,x}-\eta_1\psi_x\right)+Z_4=\bar{I}_2\ddot{\psi}_x-\bar{I}_1\ddot{u},
\end{aligned}
\tag{22d}
$$

$$
\begin{aligned}
&-\kappa\left(b_{12}+b_{55}\right)u_{,xy}-b_{11}\kappa^2 v_{,yy}-b_{55}v_{,xx}+\kappa\left(d_{55}+d_{12}\right)\psi_{x,xy}+\kappa^2 d_{11}\psi_{y,yy}+d_{55}\psi_{y,xx}\\
&+\beta\left(-\kappa\left(b_{55}u_{,xxxy}-d_{55}\psi_{x,xxxy}\right)-\kappa^3\left(b_{55}u_{,xyyy}-d_{55}\psi_{x,xyyy}\right)+\left(b_{55}v_{,xxxx}-d_{55}\psi_{y,xxxx}\right)\right)\\
&+\beta\left(\kappa^2\left(b_{55}v_{,xxyy}-d_{55}\psi_{y,xxyy}\right)+a_{55}\kappa\eta_1\left(w_{,xxy}+\kappa^2 w_{,yyy}\right)\right)\\
&+a_{55}\ell^2\left(-\frac{3\kappa}{4}\psi_{x,xy}+\psi_{y,xx}+\frac{\kappa^2}{4}\psi_{y,yy}\right)+K_S a_{55}\eta_1\left(\kappa w_{,y}-\eta_1\psi_y\right)+Z_5=\bar{I}_2\ddot{\psi}_y-\bar{I}_1\ddot{v}\partial.
\end{aligned}
\tag{22e}
$$

where

$$
Z_1=\left(a_{11}w_{,x}w_{,xx}+\left(a_{12}+a_{55}\right)\kappa^2 w_{,y}w_{,xy}+a_{55}\kappa^2 w_{,x}w_{,yy}\right)/\eta_1, \tag{23a}
$$

$$
Z_2=\left(a_{11}\kappa^3 w_{,y}w_{,yy}+\left(a_{12}+a_{55}\right)\kappa w_{,x}w_{,xy}+a_{55}\kappa w_{,y}w_{,xx}\right)/\eta_1, \tag{23b}
$$

$$
\begin{aligned}
Z_3=&\left(\bar{N}_{xx}w_{,xx}+2\kappa\bar{N}_{xy}w_{,xy}+\kappa^2\bar{N}_{yy}w_{,yy}\right)\Big/\eta_1\\
&+\left(\bar{N}_{xx,x}w_{,x}+\kappa\bar{N}_{xy,x}w_{,y}+\kappa\bar{N}_{xy,y}w_{,x}+\kappa^2\bar{N}_{yy,y}w_{,y}\right)\Big/\eta_1,
\end{aligned}
\tag{23c}
$$

$$
Z_4=\left(b_{11}w_{,x}w_{,xx}+\left(b_{12}+b_{55}\right)\kappa^2 w_{,y}w_{,xy}+b_{55}\kappa^2 w_{,x}w_{,yy}\right)/\eta_1, \tag{23d}
$$

$$
Z_5=\left(b_{11}\kappa^3 w_{,y}w_{,yy}+\left(b_{12}+b_{55}\right)\kappa w_{,x}w_{,xy}+b_{55}\kappa w_{,y}w_{,xx}\right)/\eta_1, \tag{23e}
$$

$$
\bar{N}_{xx}=a_{11}\left(u_{,x}+\frac{1}{2\eta_1}w_{,x}^2\right)-b_{11}\psi_{x,x}+a_{12}\kappa\left(v_{,y}+\frac{1}{2\eta_2}\partial w_{,y}^2\right)-b_{12}\kappa\psi_{y,y}, \tag{23f}
$$

$$
\bar{N}_{yy}=a_{11}\kappa\left(v_{,y}+\frac{1}{2\eta_2}\partial w_{,y}^2\right)-b_{11}\kappa\psi_{y,y}+a_{12}\left(u_{,x}+\frac{1}{2\eta_1}w_{,x}^2\right)-b_{12}\psi_{x,x}, \tag{23g}
$$

$$
\bar{N}_{xy}=a_{55}\left(\kappa u_{,y}+v_{,x}+\frac{\kappa}{\eta_1}w_{,x}w_{,y}\right)-b_{55}\left(\kappa\psi_{x,y}+\psi_{y,x}\right). \tag{23h}
$$

3 SOLUTION STRATEGY

Prior to go through the free vibration of buckled FG microplates, the postbuckling behavior must be investigated. To approach this purpose, we solve the nonlinear governing equations in the absence of time-dependent terms. To discretize the governing equations along with boundary conditions, the GDQ (Shu et al. 2000) method, an efficient method to solve the set of nonlinear partial

differential equations, is used. According to this method, a variable function, $\mathrm{f}(x)$, on the domain $[x_1,\ldots,x_N]$ is defined of which rth-order derivative of $\mathrm{f}(\mathrm{X})$ at a given point $\mathrm{X_i}$ can be approximated by

$$\frac{\mathrm{d}^{\mathrm{r}}\mathrm{f}(x)}{\mathrm{d}x^{\mathrm{r}}}=\sum_{\mathrm{j}=1}^{\mathrm{N}}\mathbf{D}_{\xi}^{(\mathrm{r})}\mathrm{f}\left(x_{\mathrm{j}}\right). \tag{24}$$

in which $\mathrm{D}_{\xi}^{(\mathrm{r})}$ stands for the weighting coefficients of rth-order derivative and is defined as

$$\mathbf{D}_{\xi}^{(\mathrm{r})}=\left[\mathcal{W}_{\mathrm{ij}}^{(\mathrm{r})}\right],\ i,j=1,2,\ldots,N \quad \text{and} \quad r=0,1,2,\ldots,N-1. \tag{25a}$$

$$\mathcal{W}_{\mathrm{ij}}^{(\mathrm{r})}=\begin{cases}\mathbf{I} & \mathrm{r}=0\\ \dfrac{\mathcal{P}\left(x_{\mathrm{i}}\right)}{\left(x_{\mathrm{i}}-x_{\mathrm{j}}\right)\mathcal{P}\left(\mathrm{x_j}\right)} & \mathrm{i,j=\ 1,\ldots,N\ and\ i\neq j\ and\ r=1}\\ \begin{cases} r\left[\mathcal{W}_{\mathrm{ij}}^{(1)}\mathcal{W}_{\mathrm{ii}}^{(\mathrm{r}-1)}-\dfrac{\mathcal{W}_{\mathrm{ij}}^{(\mathrm{r}-1)}}{x_{\mathrm{i}}-x_{\mathrm{j}}}\right], & i\neq j\\ -\displaystyle\sum_{k=1,k\neq i}^{\mathrm{N}}\mathcal{W}_{\mathrm{ik}}^{(\mathrm{r})}, & i=j\end{cases} & \mathrm{i,j=1,\ldots,N\ and\ r\geq 2}\end{cases} \tag{25b}$$

where $\mathcal{P}\left(x_{\mathrm{i}}\right)=\prod_{\mathrm{k=1;\ i\neq k}}^{\mathrm{N}}\left(x_{\mathrm{i}}-x_{\mathrm{k}}\right)$ and $\mathbf{I}$ is a $\mathrm{N}\times\mathrm{N}$ identity matrix.

To accommodate the GDQ technique to a two-dimensional case, the Kronecker tensor product indicated by $\otimes$ is used to approximate the partial derivative of a two variable function $\mathrm{f}(x,y)$ defined on $[x_1,\ldots,x_N]$ and $[y_1,\ldots,y_M]$. Therefore, the second order partial derivative of $\mathrm{f}(x,y)$ with respect to x and y can be written as

$$\frac{\partial^2\mathrm{f}(x,y)}{\partial x\partial y}=\left(\mathbf{D}_{y}^{(1)}\otimes\mathbf{D}_{x}^{(1)}\right)\overline{\mathbf{f}}. \tag{26}$$

where $\overline{\mathrm{f}}$ is a column vector introduced as

$$\overline{\mathbf{f}}=\left[\mathrm{f}(x_1,y_1),\ldots,\ \mathrm{f}(x_{\mathrm{N}},y_1),\mathrm{f}(x_1,y_2),\ldots,\mathrm{f}(x_{\mathrm{N}},y_2),\ldots,\mathrm{f}(x_1,y_{\mathrm{M}}),\ldots,\mathrm{f}(x_{\mathrm{N}},y_{\mathrm{M}})\right]^{\mathrm{T}}. \tag{27}$$

In order to generate grid points in the X and Y directions, the shifted Chebyshev–Gauss–Lobatto grid points can be employed

$$\begin{aligned} x_{\mathrm{i}}&=\frac{1}{2}\left(1-\cos\frac{\mathrm{i}-1}{\mathrm{N}-1}\pi\right), \qquad \mathrm{i}=1,2,\ldots,\mathrm{N}\\ y_{\mathrm{j}}&=\frac{1}{2}\left(1-\cos\frac{\mathrm{j}-1}{\mathrm{M}-1}\pi\right), \qquad \mathrm{j}=1,2,\ldots,\mathrm{M}. \end{aligned} \tag{28}$$

Considering postbuckling problem, the external forces are $\overline{\mathrm{N}}^0_{\mathrm{xx}}=-\gamma_1\mathrm{P}, \overline{\mathrm{N}}^0_{\mathrm{yy}}=-\gamma_2\mathrm{P}$ and $\overline{\mathrm{N}}^0_{\mathrm{xy}}=0$. Neglecting the time-dependent terms in the governing equations and writing the discretized forms result in following equation

$$\left(\mathbf{K}-\mathrm{P}\mathbf{K}_{\mathrm{g}}\right)\mathbf{X}_{\mathrm{s}}+\mathbf{R}\left(\mathbf{X}_{\mathrm{s}}\right)=0 \tag{29}$$

in which $\mathbf{X}_{\mathrm{s}}=\left\{\overline{\mathbf{u}}_{\mathrm{s}},\overline{\mathbf{v}}_{\mathrm{s}},\overline{\mathbf{w}}_{\mathrm{s}},\overline{\boldsymbol{\psi}}_{\mathrm{x}_s},\overline{\boldsymbol{\psi}}_{\mathrm{y}_s}\right\}^{\mathrm{T}}, \mathbf{R}\left(\mathbf{X}_{\mathrm{s}}\right)=\left\{\mathbf{R}_1,\mathbf{R}_2,\ \mathbf{R}_3,\mathbf{R}_4,\mathbf{R}_5\right\}^{\mathrm{T}}$ and the column vectors of the displacement variables in the postbuckling region including $\overline{\mathbf{u}}_{\mathrm{s}},\overline{\mathbf{v}}_{\mathrm{s}},\overline{\mathbf{w}}_{\mathrm{s}},\overline{\boldsymbol{\psi}}_{\boldsymbol{x}_s}$ and $\overline{\boldsymbol{\psi}}_{\mathrm{y}_s}$ with NM elements are defined as

$$\overline{\mathbf{u}}_{\mathrm{s}}=\left[\mathrm{u}(x_1,y_1),\ldots,\ \mathrm{u}(x_{\mathrm{N}},y_1),\mathrm{u}(x_1,y_2),\ldots,\mathrm{u}(x_{\mathrm{N}},y_2),\ldots,\mathrm{u}(x_1,y_{\mathrm{M}}),\ldots,\mathrm{u}(x_{\mathrm{N}},y_{\mathrm{M}})\right]^{\mathrm{T}}, \tag{30a}$$

$$\overline{\mathbf{v}}_{\mathrm{s}}=\left[\mathrm{v}(x_1,y_1),\ldots,\ \mathrm{v}(x_{\mathrm{N}},y_1),\mathrm{v}(x_1,y_2),\ldots,\mathrm{v}(x_{\mathrm{N}},y_2),\ldots,\mathrm{v}(x_1,y_{\mathrm{M}}),\ldots,\mathrm{v}(x_{\mathrm{N}},y_{\mathrm{M}})\right]^{\mathrm{T}}, \tag{30b}$$

$$\overline{\mathbf{w}}_{\mathrm{s}}=\left[\mathrm{w}(x_1,y_1),\ldots,\mathrm{w}(x_{\mathrm{N}},y_1),\mathrm{w}(x_1,y_2),\ldots,\mathrm{w}(x_{\mathrm{N}},y_2),\ldots,\mathrm{w}(x_1,y_{\mathrm{M}}),\ldots,\mathrm{w}(x_{\mathrm{N}},y_{\mathrm{M}})\right]^{\mathrm{T}}, \tag{30c}$$

$$\overline{\boldsymbol{\psi}}_{\mathrm{x}_s}=\left[\psi_{\mathrm{x}}(x_1,y_1),\ldots,\ \psi_{\mathrm{x}}(x_{\mathrm{N}},y_1),\psi_{\mathrm{x}}(x_1,y_2),\ldots,\psi_{\mathrm{x}}(x_{\mathrm{N}},y_2),\ldots,\psi_{\mathrm{x}}(x_1,y_{\mathrm{M}}),\ldots,\psi_{\mathrm{x}}(x_{\mathrm{N}},y_{\mathrm{M}})\right]^{\mathrm{T}}, \tag{30d}$$

$$\overline{\boldsymbol{\psi}}_{\mathrm{y}_s}=\left[\psi_{\mathrm{y}}(x_1,y_1),\ldots,\ \psi_{\mathrm{y}}(x_{\mathrm{N}},y_1),\psi_{\mathrm{y}}(x_1,y_2),\ldots,\psi_{\mathrm{y}}(x_{\mathrm{N}},y_2),\ldots,\psi_{\mathrm{y}}(x_1,y_{\mathrm{M}}),\ldots,\psi_{\mathrm{y}}(x_{\mathrm{N}},y_{\mathrm{M}})\right]^{\mathrm{T}} \tag{30e}$$

Also,

$$\mathbf{K}=\begin{bmatrix}\mathbf{K}_{11} & \mathbf{K}_{12} & \mathbf{K}_{13} & \mathbf{K}_{14} & \mathbf{K}_{15}\\ \mathbf{K}_{21} & \mathbf{K}_{22} & \mathbf{K}_{23} & \mathbf{K}_{24} & \mathbf{K}_{25}\\ \mathbf{K}_{31} & \mathbf{K}_{32} & \mathbf{K}_{33} & \mathbf{K}_{34} & \mathbf{K}_{35}\\ \mathbf{K}_{41} & \mathbf{K}_{42} & \mathbf{K}_{43} & \mathbf{K}_{44} & \mathbf{K}_{45}\\ \mathbf{K}_{51} & \mathbf{K}_{52} & \mathbf{K}_{53} & \mathbf{K}_{54} & \mathbf{K}_{55}\end{bmatrix},$$

$$\mathbf{K}_{\mathrm{g}}=\begin{bmatrix}\mathbf{0} & \mathbf{0} & \mathbf{0} & \mathbf{0} & \mathbf{0}\\ \mathbf{0} & \mathbf{0} & \mathbf{0} & \mathbf{0} & \mathbf{0}\\ \mathbf{0} & \mathbf{0} & \left(\mathbf{I}_y\otimes\mathbf{D}_x^{(2)}\right)\gamma_1+\kappa^2\left(\mathbf{D}_y^{(2)}\otimes\mathbf{I}_x\right)\gamma_2 & \mathbf{0} & \mathbf{0}\\ \mathbf{0} & \mathbf{0} & \mathbf{0} & \mathbf{0} & \mathbf{0}\\ \mathbf{0} & \mathbf{0} & \mathbf{0} & \mathbf{0} & \mathbf{0}\end{bmatrix}. \tag{31}$$

where $\mathbf{I}_y$ and $\mathbf{I}_x$ are $M\times M$ and $N\times N$ identity tensors, respectively.The definitions of the components of stiffness matrix $\mathbf{K}$ can be found in appendix A. Also, in appendix B, $\mathbf{R}_1,\mathbf{R}_2,\mathbf{R}_3,\mathbf{R}_4$ and $\mathbf{R}_5$ including the nonlinear terms are represented. If the nonlinear terms vanish, Eq. (29) declines to an eigenvalue problem as $\left[\mathbf{K}-\mathrm{P}\mathbf{K}_{\mathrm{g}}\right]\mathbf{X}_{\mathrm{s}}=\mathbf{0}$ which gives the critical buckling load of FG microplate and corresponding mode shapes. Eq. (29) can be written in the form of a system of parameterized nonlinear equations as

$$\mathbf{F}\left(\mathbf{X}_{\mathrm{s}},\mathrm{P}\right)=\mathbf{K}\mathbf{X}_{\mathrm{s}}-\mathrm{P}\mathbf{K}_{\mathrm{g}}\mathbf{X}_{\mathrm{s}}+\mathbf{R}\left(\mathbf{X}_{\mathrm{s}}\right)=\mathbf{0}. \tag{32}$$

To find the solution of this parameterized problem, one can employ the Pseudo-arclength continuation (Keller 1977). With regards to this method, via an iterative solver, an additional constraint is added to the system of nonlinear equations to find a point at the given pseudo-arclength. The resulting augmented system can be written as

$$\begin{cases} F\left(\mathbf{X}_{\mathrm{s}},\mathrm{P}\right)=0\\ \dot{\mathbf{X}}_0\left(\mathbf{X}_{\mathrm{s}}-\mathbf{X}_0\right)+\dot{\lambda}_0\left(\mathrm{P}-\mathrm{P}_0\right)=\Delta s\end{cases}. \tag{33}$$

where $\left(\mathbf{X}_0,\mathrm{P}_0\right)$ is the initial solution and $\left(\dot{\mathbf{X}}_0,\dot{\mathrm{P}}_0\right)$ is the tangent vector of the solution path at $\left(\mathbf{X}_0,\mathrm{P}_0\right)$. $\Delta\mathrm{s}$ represents the step-size used in predicting the next points. The next points are selected in a step $\Delta\mathrm{s}$ along the tangent vector at the current point. Afterwards, to improve the point predicted in the first stage, by supposing the initial guess as the linear solution of the system and using the Newton method, the above nonlinear system can be solved. Eq. (33) leads to a square Jacobian as

$$\mathbf{J}=\begin{bmatrix}\left[\dfrac{\partial \mathbf{F}}{\partial \mathbf{X}_{\mathrm{s}}}=\left(\mathbf{K}-\mathrm{P}\mathbf{K}_{\mathrm{g}}+\dfrac{\partial \mathbf{R}}{\partial \mathbf{X}_{\mathrm{s}}}\right)\right] & \left[\dfrac{\partial \mathbf{F}}{\partial \mathrm{P}}=-\mathbf{K}_{\mathrm{g}}\mathbf{X}_{\mathrm{s}}\right] \\ \left[\dot{\mathbf{X}}_0\right] & \dot{\lambda}_0\end{bmatrix}. \tag{34}$$

Considering $\mathbf{J}\dot{\mathbf{V}}=\begin{Bmatrix}0\\1\end{Bmatrix}$, the tangent vector $\dot{\mathbf{V}}=\begin{Bmatrix}\dot{\mathbf{X}}_s\\ \dot{\mathrm{P}}\end{Bmatrix}$ related to the subsequent steps can be obtained.

So as to investigate the free vibration of the microplate around the buckled configuration, we need to introduce a small disturbance depending on time. The displacement vector $\mathbf{X}=\left\{\overline{\mathbf{u}},\overline{\mathbf{v}},\overline{\mathbf{w}},\overline{\boldsymbol{\psi}}_{\mathrm{x}},\overline{\boldsymbol{\psi}}_{\mathrm{y}}\right\}^{\mathrm{T}}$ includes both the buckled configuration and the dynamic disturbance (Li et al. 2004; Li et al. 2007)

$$\mathbf{X}=\mathbf{X}_{\mathrm{s}}+\mathrm{d}\mathbf{X}_{\mathrm{d}}. \tag{35}$$

By employing Eq. (35), the discretized nonlinear governing equations including the time-dependent terms can be written as

$$\mathbf{F}\left(\mathbf{X},\mathrm{P}\right)=\mathbf{K}\mathbf{X}-\mathrm{P}\mathbf{K}_{\mathrm{g}}\mathbf{X}+\mathbf{R}\left(\mathbf{X}\right)+\mathbf{M}\ddot{\mathbf{X}}=\mathbf{0}. \tag{36}$$

in which $\ddot{\mathbf{X}}$ is the second derivative of $\mathbf{X}$ with respect to time and

$$\mathbf{M}=\begin{bmatrix}\overline{\mathrm{I}}_0\left(\mathbf{I}_y\otimes\mathbf{I}_x\right) & \mathbf{0} & \mathbf{0} & -\overline{\mathrm{I}}_2\left(\mathbf{I}_y\otimes\mathbf{I}_x\right) & \mathbf{0}\\ \mathbf{0} & \overline{\mathrm{I}}_0\left(\mathbf{I}_y\otimes\mathbf{I}_x\right) & \mathbf{0} & \mathbf{0} & -\overline{\mathrm{I}}_1\left(\mathbf{I}_y\otimes\mathbf{I}_x\right)\\ \mathbf{0} & \mathbf{0} & \overline{\mathrm{I}}_0\left(\mathbf{I}_y\otimes\mathbf{I}_x\right) & \mathbf{0} & \mathbf{0}\\ -\overline{\mathrm{I}}_1\left(\mathbf{I}_y\otimes\mathbf{I}_x\right) & \mathbf{0} & \mathbf{0} & \overline{\mathrm{I}}_2\left(\mathbf{I}_y\otimes\mathbf{I}_x\right) & \mathbf{0}\\ \mathbf{0} & -\overline{\mathrm{I}}_1\left(\mathbf{I}_y\otimes\mathbf{I}_x\right) & \mathbf{0} & \mathbf{0} & \overline{\mathrm{I}}_2\left(\mathbf{I}_y\otimes\mathbf{I}_x\right)\end{bmatrix}. \tag{37}$$

Considering Eq. (35) and Eq. (36), and using Taylor's expansion about $\mathbf{X}_{\mathrm{s}}$ gives

$$\mathbf{F}\left(\mathbf{X}_{\mathrm{s}}+\mathrm{d}\mathbf{X}_{\mathrm{d}},\lambda\right)=\mathbf{F}\left(\mathbf{X}_{\mathrm{s}},\lambda\right)+\left.\frac{\partial \mathbf{F}}{\partial \mathbf{X}}\right|_{\mathbf{X}=\mathbf{X}_{\mathrm{s}}}\mathrm{d}\mathbf{X}_{\mathrm{d}}+\mathbf{H.O.T}=\mathbf{0}. \tag{38}$$

Given the dynamic disturbances are negligible compared to the postbuckling configuration, the higher order terms $\mathbf{H.O.T}$ can be neglected. So, using Eqs. (36) and (38) gives

$$\mathbf{F}\left(\mathbf{X}_{\mathrm{s}}+\mathrm{d}\mathbf{X}_{\mathrm{d}},\mathrm{P}\right)=\left.\frac{\partial \mathbf{F}}{\partial \mathbf{X}}\right|_{\mathbf{X}=\mathbf{X}_{\mathrm{s}}}\mathrm{d}\mathbf{X}_{\mathrm{d}}=\left(\mathbf{K}-\mathrm{P}\mathbf{K}_{\mathrm{g}}+\frac{\partial \mathbf{R}}{\partial \mathbf{X}_{\mathrm{s}}}\right)\mathrm{d}\mathbf{X}_{\mathrm{d}}-\mathbf{M}\mathrm{d}\ddot{\mathbf{X}}_{d}=\mathbf{0}. \tag{39}$$

By considering $\mathbf{dX}_{\mathrm{d}} = \left\{ \bar{\boldsymbol{\delta}}_{\mathbf{u}} \bar{\boldsymbol{\delta}}_{\mathbf{v}} \bar{\boldsymbol{\delta}}_{\mathbf{w}} \bar{\boldsymbol{\delta}}_{\psi_x} \bar{\boldsymbol{\delta}}_{\psi_y} \right\}^{\mathrm{T}} \mathrm{e}^{\mathrm{i}\omega\tau}$, where ω is the non-dimensional natural frequency, and assuming $\bar{\boldsymbol{\delta}}_{\mathbf{u}}$, $\bar{\boldsymbol{\delta}}_{\mathbf{v}}$, $\bar{\boldsymbol{\delta}}_{\mathbf{w}}$, $\bar{\boldsymbol{\delta}}_{\psi_x}$ and $\bar{\boldsymbol{\delta}}_{\psi_y}$ as column vectors of NM elements representing the associated mode shapes, equation (36) can be expressed as

$$\left(\bar{\mathbf{K}} - \omega^2 \mathbf{M} \right) \mathbf{X}_{\mathrm{d}} = 0. \tag{40}$$

where $\mathbf{X}_{\mathrm{d}} = \left\{ \bar{\boldsymbol{\delta}}_{\mathbf{u}} \bar{\boldsymbol{\delta}}_{\mathbf{v}} \bar{\boldsymbol{\delta}}_{\mathbf{w}} \bar{\boldsymbol{\delta}}_{\psi_x} \bar{\boldsymbol{\delta}}_{\psi_y} \right\}^{\mathrm{T}}$ and

$$\bar{\mathbf{K}} = \frac{\partial \mathbf{F}}{\partial \mathbf{X}_{\mathrm{s}}} = \left(\mathbf{K} - \mathrm{P}\mathbf{K}_{\mathrm{g}} + \frac{\partial \mathbf{R}}{\partial \mathbf{X}_{\mathrm{s}}} \right), \quad \frac{\partial \mathbf{R}}{\partial \mathbf{X}_{\mathrm{s}}} = \begin{bmatrix} \frac{\partial \mathbf{R}_1}{\partial \bar{\mathbf{u}}_{\mathrm{s}}} & \frac{\partial \mathbf{R}_1}{\partial \bar{\mathbf{v}}_{\mathrm{s}}} & \frac{\partial \mathbf{R}_1}{\partial \bar{\mathbf{w}}_{\mathrm{s}}} & \frac{\partial \mathbf{R}_1}{\partial \bar{\boldsymbol{\psi}}_{\mathrm{x}_s}} & \frac{\partial \mathbf{R}_1}{\partial \bar{\boldsymbol{\psi}}_{\mathrm{y}_s}} \\ \frac{\partial \mathbf{R}_2}{\partial \bar{\mathbf{u}}_{\mathrm{s}}} & \frac{\partial \mathbf{R}_2}{\partial \bar{\mathbf{v}}_{\mathrm{s}}} & \frac{\partial \mathbf{R}_2}{\partial \bar{\mathbf{w}}_{\mathrm{s}}} & \frac{\partial \mathbf{R}_2}{\partial \bar{\boldsymbol{\psi}}_{\mathrm{x}_s}} & \frac{\partial \mathbf{R}_2}{\partial \bar{\boldsymbol{\psi}}_{\mathrm{y}_s}} \\ \frac{\partial \mathbf{R}_3}{\partial \bar{\mathbf{u}}_{\mathrm{s}}} & \frac{\partial \mathbf{R}_3}{\partial \bar{\mathbf{v}}_{\mathrm{s}}} & \frac{\partial \mathbf{R}_3}{\partial \bar{\mathbf{w}}_{\mathrm{s}}} & \frac{\partial \mathbf{R}_3}{\partial \bar{\boldsymbol{\psi}}_{\mathrm{x}_s}} & \frac{\partial \mathbf{R}_3}{\partial \bar{\boldsymbol{\psi}}_{\mathrm{y}_s}} \\ \frac{\partial \mathbf{R}_4}{\partial \bar{\mathbf{u}}_{\mathrm{s}}} & \frac{\partial \mathbf{R}_4}{\partial \bar{\mathbf{v}}_{\mathrm{s}}} & \frac{\partial \mathbf{R}_4}{\partial \bar{\mathbf{w}}_{\mathrm{s}}} & \frac{\partial \mathbf{R}_4}{\partial \bar{\boldsymbol{\psi}}_{\mathrm{x}_s}} & \frac{\partial \mathbf{R}_4}{\partial \bar{\boldsymbol{\psi}}_{\mathrm{y}_s}} \\ \frac{\partial \mathbf{R}_5}{\partial \bar{\mathbf{u}}_{\mathrm{s}}} & \frac{\partial \mathbf{R}_5}{\partial \bar{\mathbf{v}}_{\mathrm{s}}} & \frac{\partial \mathbf{R}_5}{\partial \bar{\mathbf{w}}_{\mathrm{s}}} & \frac{\partial \mathbf{R}_5}{\partial \bar{\boldsymbol{\psi}}_{\mathrm{x}_s}} & \frac{\partial \mathbf{R}_5}{\partial \bar{\boldsymbol{\psi}}_{\mathrm{y}_s}} \end{bmatrix} \tag{41}$$

It is noteworthy to mention that the stiffness matrix achieved corresponding to the free vibration of the buckled microplate is equal to the first block of Jacobian matrix in Eq. (39) with the converged displacement, which was used in dealing with the postbuckling problem. Edge conditions can be imposed directly by inserting all the boundary conditions into Eq. (40). In order to convert the governing equations given by (40) to a generalized eigenvalue problem, let define the following displacement vectors $\mathbf{x}_{\mathrm{d}}$ and $\mathbf{x}_{\mathrm{b}}$ as

$$\begin{aligned} \mathbf{x}_{\mathrm{d}} &= \left\{ \left(\bar{\boldsymbol{\delta}}_{\mathbf{u}} \right)_{\mathrm{d}}^{\mathrm{T}}, \left(\bar{\boldsymbol{\delta}}_{\mathbf{v}} \right)_{\mathrm{d}}^{\mathrm{T}}, \left(\bar{\boldsymbol{\delta}}_{\mathbf{w}} \right)_{\mathrm{d}}^{\mathrm{T}}, \left(\bar{\boldsymbol{\delta}}_{\psi_x} \right)_{\mathrm{d}}^{\mathrm{T}}, \left(\bar{\boldsymbol{\delta}}_{\psi_y} \right)_{\mathrm{d}}^{\mathrm{T}} \right\}^{\mathrm{T}}, \\ \mathbf{x}_{\mathrm{b}} &= \left\{ \left(\bar{\boldsymbol{\delta}}_{\mathbf{u}} \right)_{\mathrm{b}}^{\mathrm{T}}, \left(\bar{\boldsymbol{\delta}}_{\mathbf{v}} \right)_{\mathrm{b}}^{\mathrm{T}}, \left(\bar{\boldsymbol{\delta}}_{\mathbf{w}} \right)_{\mathrm{b}}^{\mathrm{T}}, \left(\bar{\boldsymbol{\delta}}_{\psi_x} \right)_{\mathrm{b}}^{\mathrm{T}}, \left(\bar{\boldsymbol{\delta}}_{\psi_y} \right)_{\mathrm{b}}^{\mathrm{T}} \right\}^{\mathrm{T}}. \end{aligned} \tag{42}$$

in which the subscripts b and d represent the boundary and domain grid points, respectively. Accordingly, Eq. (40) can be simplified as

$$\begin{bmatrix} \mathbf{K}_{\mathrm{dd}} & \mathbf{K}_{\mathrm{db}} \\ \mathbf{K}_{\mathrm{bd}} & \mathbf{K}_{\mathrm{bb}} \end{bmatrix} \begin{Bmatrix} \mathbf{x}_{\mathrm{d}} \\ \mathbf{x}_{\mathrm{b}} \end{Bmatrix} = \omega^2 \begin{bmatrix} \mathbf{M}_{\mathrm{dd}} & \mathbf{M}_{\mathrm{db}} \\ \mathbf{0} & \mathbf{0} \end{bmatrix} \begin{Bmatrix} \mathbf{x}_{\mathrm{d}} \\ \mathbf{x}_{\mathrm{b}} \end{Bmatrix}. \tag{43}$$

Now, the eigenvalue problem in the domain can be obtained from this relation as

$$\mathbf{K}_{\mathrm{n}}\mathbf{x}_{\mathrm{d}} = -\omega^{2}\mathbf{M}_{\mathrm{n}}\mathbf{x}_{\mathrm{d}}. \tag{44}$$

where

$$\mathbf{K}_{\mathrm{n}} = \mathbf{K}_{\mathrm{dd}} - \mathbf{K}_{\mathrm{db}}\mathbf{K}_{\mathrm{bb}}^{-1}\mathbf{K}_{\mathrm{bd}}, \mathbf{M}_{\mathrm{n}} = \mathbf{M}_{\mathrm{dd}} - \mathbf{M}_{\mathrm{db}}\mathbf{K}_{\mathrm{bb}}^{-1}\mathbf{K}_{\mathrm{bd}}. \tag{45}$$

Solving Eq. (45) gives the natural frequencies of the microplate for each applied load and the associated buckled mode.

4 RESULTS AND DISCUSSION

In this part, the numerical results obtained from the MCST for the size-dependent vibration analysis of post-buckled FG Mindlin microplates with various edge supports are represented.

In order to ensure the accuracy and validity of the proposed numerical scheme, the buckling load parameters $\bar{P}_{cr} = P_{cr}a^{2}/\left(\pi^{2}D\right)$; in which $D = \left(\lambda + 2\mu\right)h^{3}/12$, for the isotropic square Mindlin microplates with various boundary conditions and subjected to equal biaxial in-plane compressive loads are calculated and compared with the results given by Zhang et al. (2013) in Table 1. The material properties are chosen as $E = 1.44GPa, \nu = 0.38, \rho = 1220kg/m^{3}$ and $l = 17.6\,\mu m$. According to this table, it can be observed that the results generated through the present solution are in good agreement with the ones reported in the literature.

Boundary conditions	Sources	Classic	$h/l=1$	$h/l=2$	$h/l=5$	$h/l=10$
CCCC	Present	5.2602	27.8230	10.1557	6.0499	5.4624
	Zhang et al.(2013)	5.2535	27.7034	10.1659	6.0617	5.4725
SSSS	Present	1.9955	9.3415	3.8499	2.2921	2.0416
	Zhang et al.(2013)	1.9928	9.3383	3.8366	2.2886	2.0669
SCSC	Present	3.8057	17.9008	7.3469	4.3761	3.9511
	Zhang et al.(2013)	3.8015	17.8973	7.3582	4.3857	3.9589

Table 1: Comparisons of buckling load parameter for isotropic homogeneous microplates with various boundary conditions and subjected to equal biaxial in-plane compressive loads $\left(a/h = 50\right)$

Afterward, the effects of the length scale parameter h/l, gradient index n, and length-to-thickness ratio a/h on the free vibration characteristics of postbuckled FG microplates are discussed in detail. It is considered that the microplates made of two materials including aluminum (Al) and ceramic (SiC) are considered with the material properties $\mathrm{E_m} = 70\ \mathrm{GPa}$ and $\nu_{\mathrm{m}} = 0.3$, for Al, and $\mathrm{E_c} = 427\ \mathrm{GPa}$ and $\nu_{\mathrm{c}} = 0.17$ for SiC. In this paper, FG microplates with three boundary conditions, including fully simply supported edges (SSSS), two opposite sides simply supported and two others clamped edges (SCSC), and fully clamped edges (CCCC) end supports are investigated.

The effect of the length scale parameter on the postbuckling deflection of FG microplates with different boundary conditions predicted by the MCST is illustrated in figure 2. An increase in the

value of non-dimensional length scale parameter shifts the postbuckling curves to the left-hand side, resulting in lower critical applied loads and higher non-dimensional deflections. In other words, the CT theory underestimates and overestimates the non-dimensional axial load and non-dimensional deflection, respectively. Given that the distance between postbuckling paths is comparatively large at microplates with CCCC edge supports, the importance of using the size-dependent MCST gets more pronounced in these microplates.

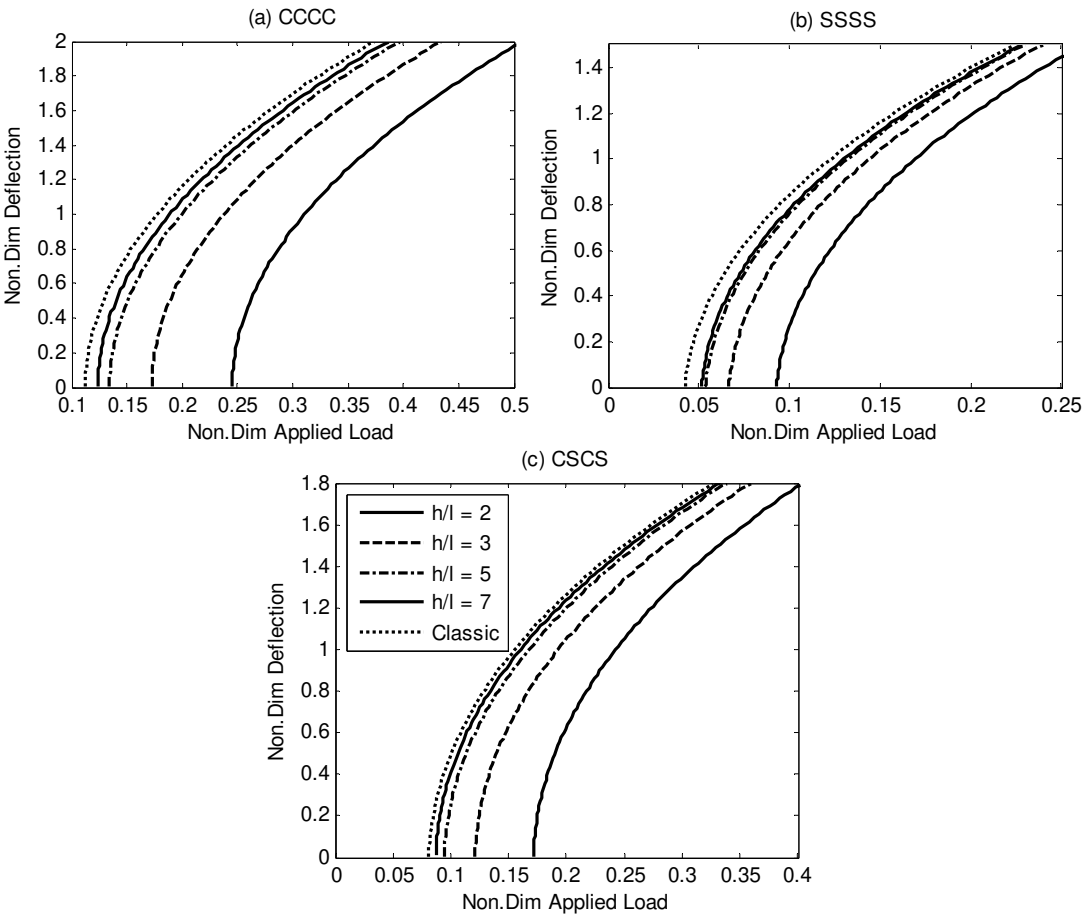

Figure 2: Effect of non-dimensional length scale parameter on non-dimensional postbuckling deflection of FG microplate for different boundary conditions $\left(n = 0.2, a/h = b/h = 12\right)$

Depicted in figures 3 is the effect of the length scale parameter on frequency-response curves of FG microplates with different boundary conditions around the undeflected and the first buckled configurations. It is seen that while microplate is in unbuckled configuration, an increase in the non-dimensional applied load decreases the non-dimensional frequency; but, when the non-dimensional axial load exceeds the critical applied load, the non-dimensional frequency grows. As long as the FG microplate is in undeflected region, an increase in the non-dimensional length scale parameter gives lower non-dimensional frequency; while, in the buckled configuration, this increment leads to the opposite result and higher non-dimensional natural frequencies.

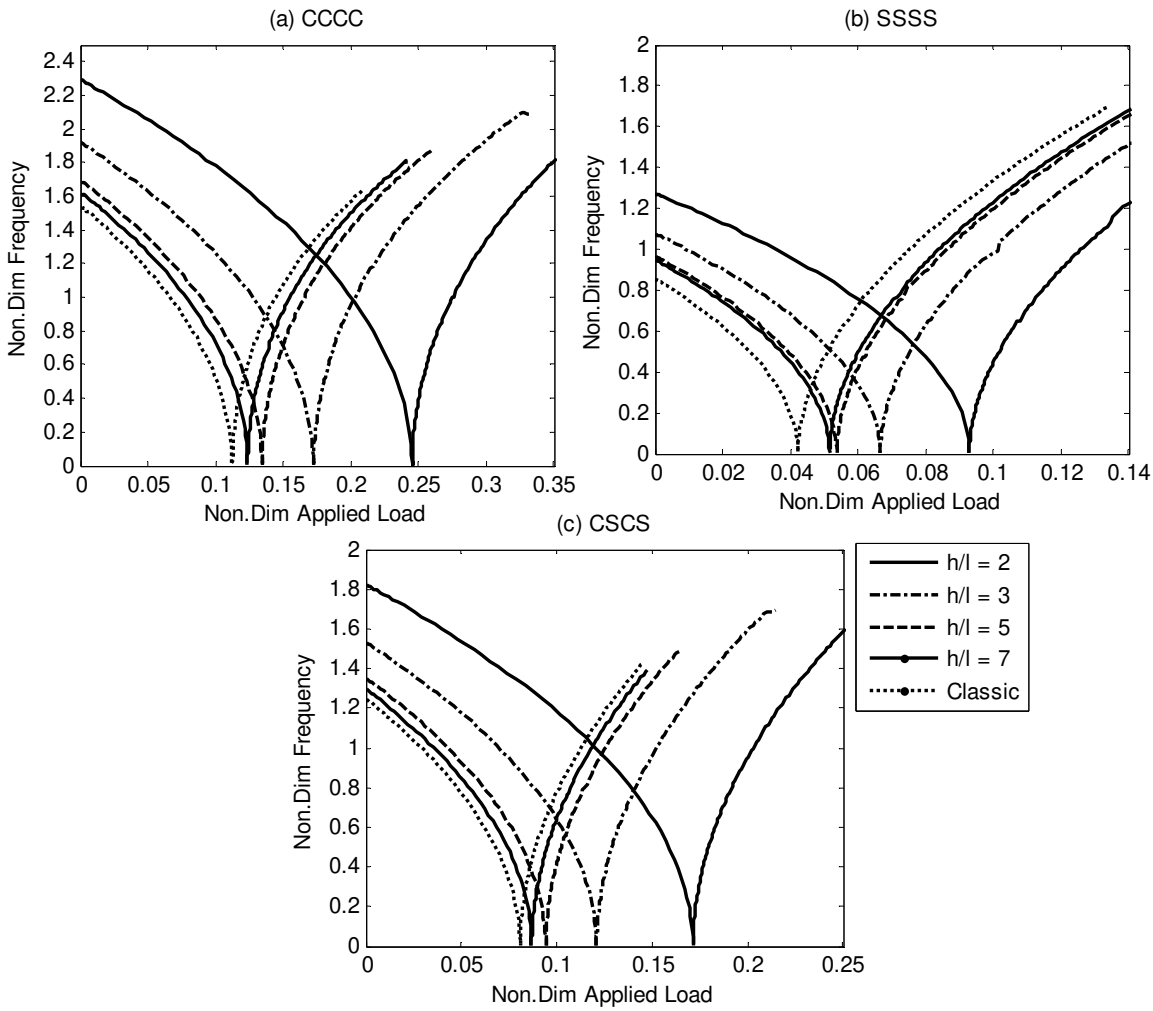

Figure 3: Non-dimensional fundamental natural frequency of the FG microplate around the undeflected and the first buckled configurations versus non-dimensional applied load for different non-dimensional length scale paramters $\left(n = 0.2, a/h = b/h = 12\right)$

The effect of the material gradient index n on the postbuckling deflection of FG microplates with CCCC, CSCS and SSSS boundary conditions is shown in figure 4. With the rise of the material gradient index, the critical applied load declines and large postbuckled deflections are induced. Moreover, it can be deduced that microplates with CCCC edge supports are more affected by the variation of material gradient index compared to other counterparts.

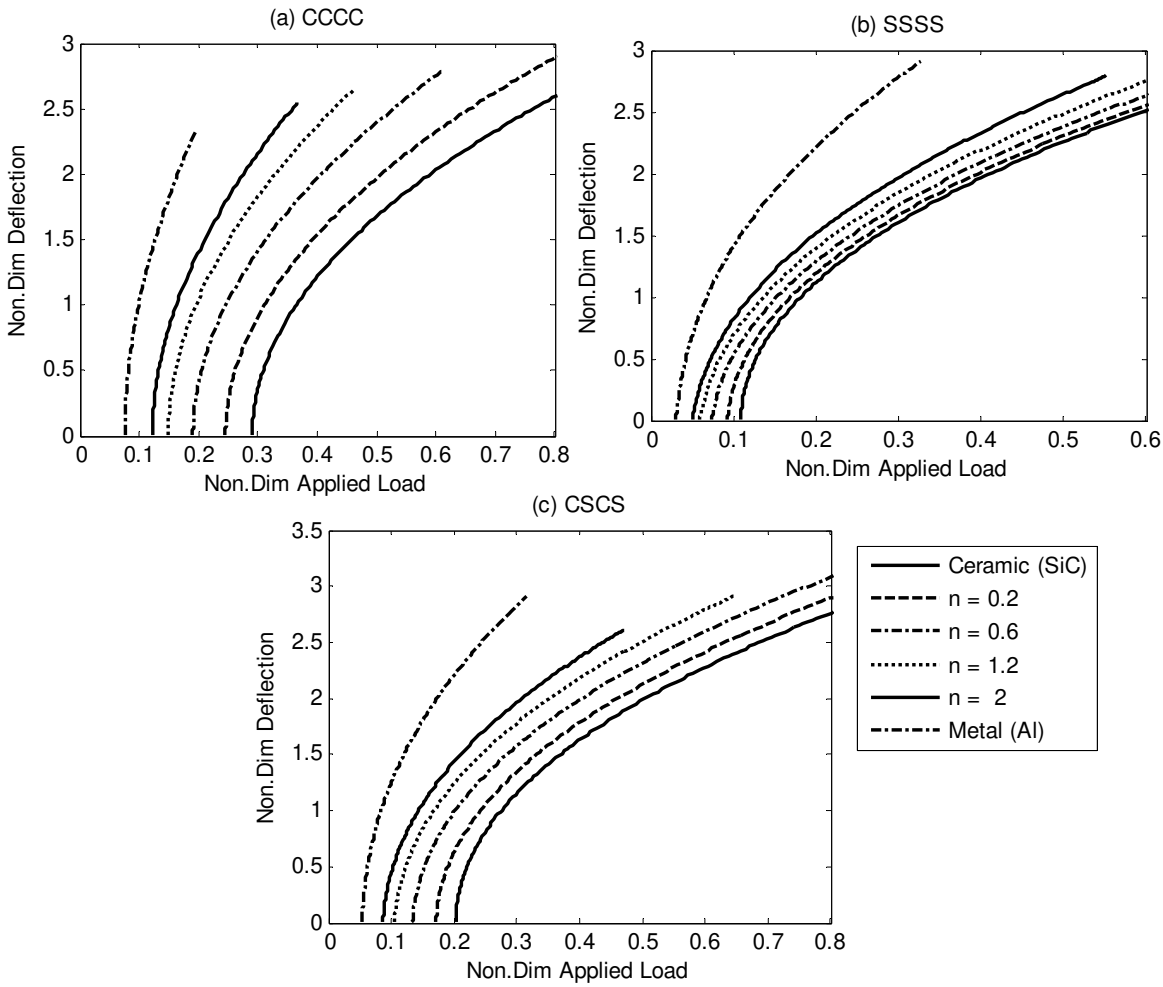

Figure 4: Effect of material gradient index on nondimensional postbuckling deflection of FG microplate for different boundary conditions $\left(\mathrm{h}/l = 2,\ \mathrm{a}/\mathrm{h} = \mathrm{b}/\mathrm{h} = 12\right)$

Figure 5 illustrates the variation of the non-dimensional natural frequency with the non-dimensional axial load for FG microplates with different material gradient indexes. With the increase of the material gradient index, the frequency-response curves move to the left-hand side inducing lower stability.

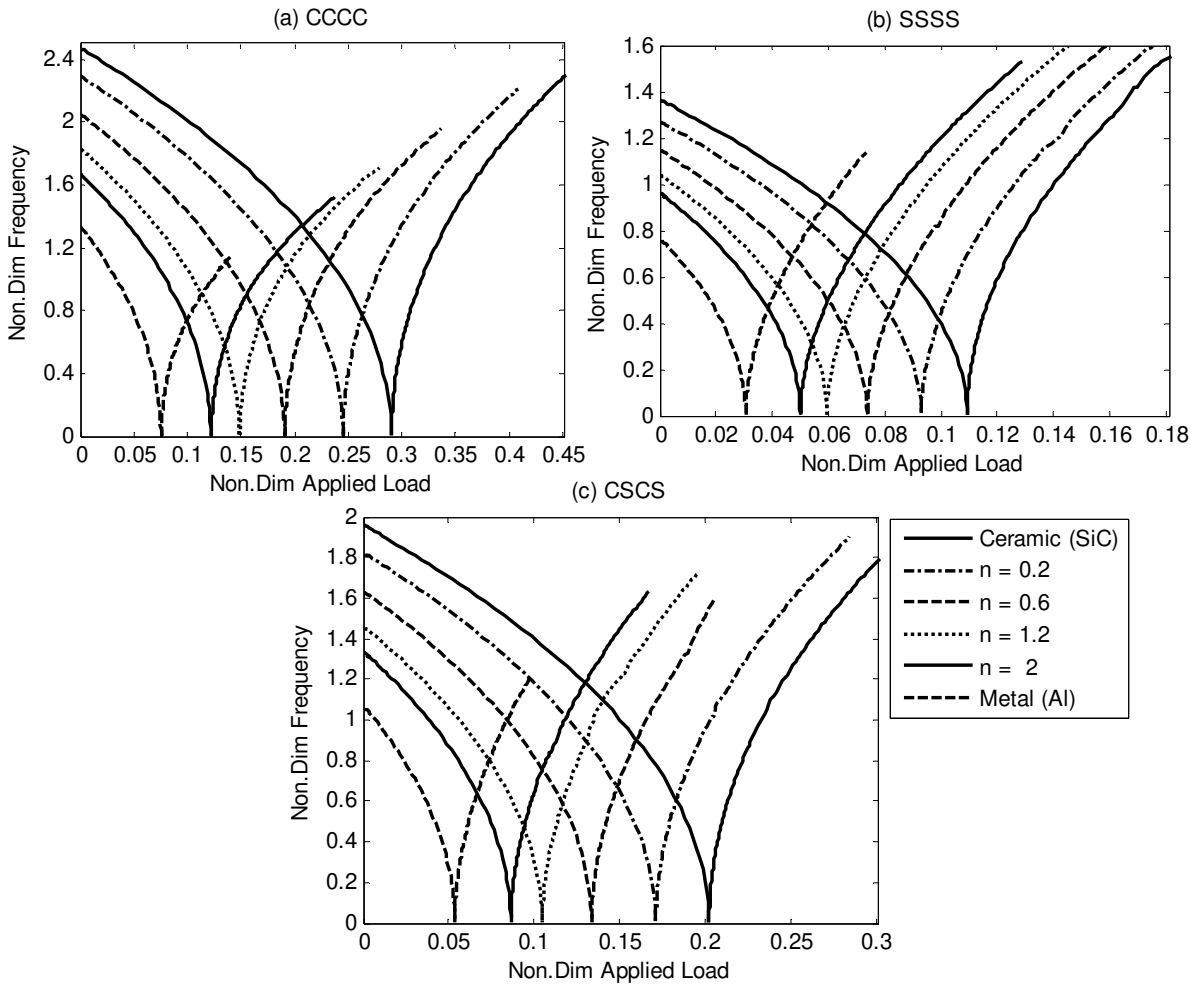

Figure 5: Non-dimensional fundamental natural frequency of the FG microplate around the undeflected and the first buckled configurations versus non-dimensional axial load for different material gradient indices $\left(\mathrm{h}/l = 2,\ \mathrm{a}/\mathrm{h} = \mathrm{b}/\mathrm{h} = 12\right)$

Figure 6 is depicted to investigate the effect of the aspect ratio on the non-dimensional postbuckling deflection of FG microplates with different boundary conditions. It can be seen that an increase in the value of aspect ratio reduces the critical buckling load and induces higher buckled deflection. The proximity of curves at microplates with SSSS edge supports indicates the pallid role of this parameter on the postbuckling path of these types of microplates.

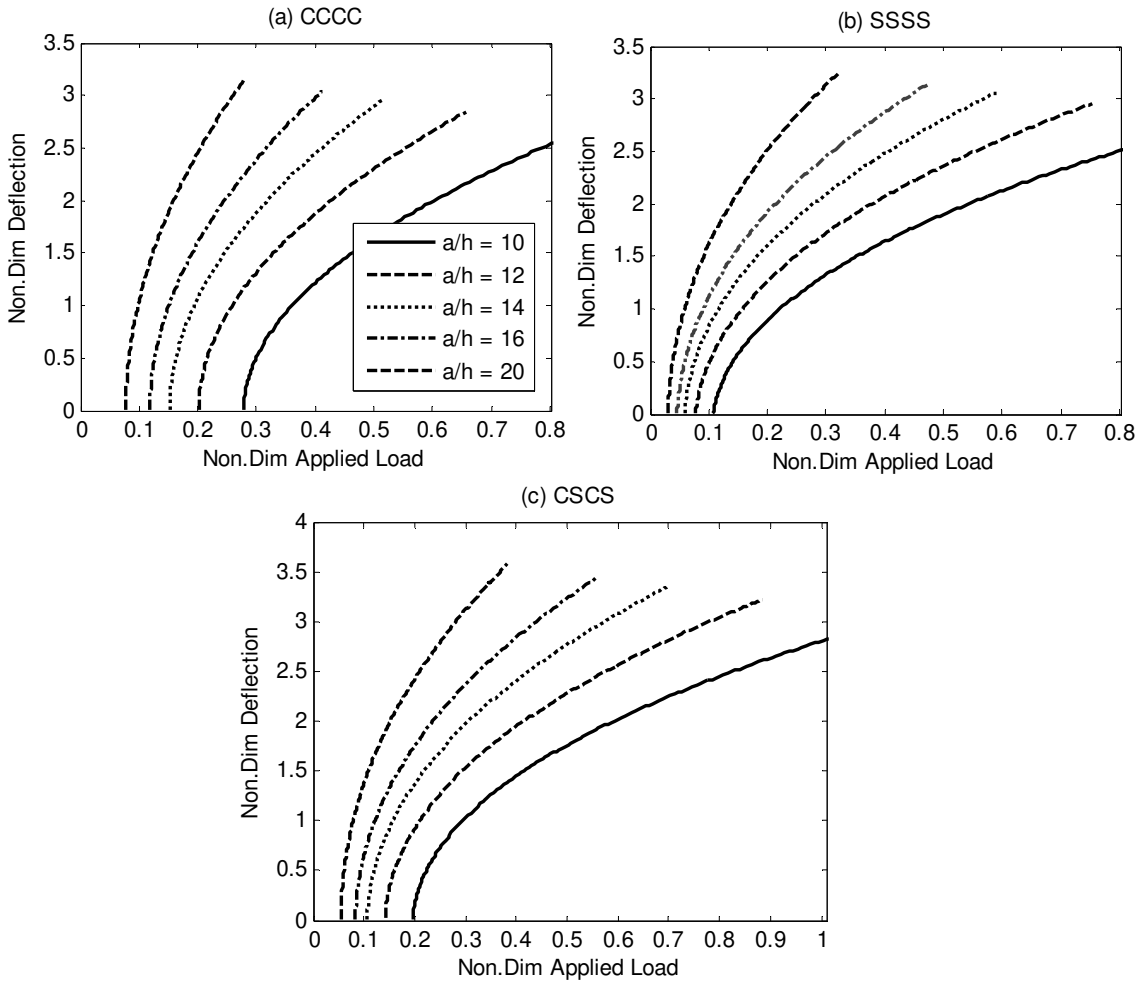

Figure 6: Effect of aspect ratio on non-dimensional postbuckling deflection of FG microplate for different boundary conditions $\left(n = 0.5, h/l = 2,\ b/a = 1\right)$

Shown in figure 7 is the variation of the non-dimensional natural frequency with the non-dimensional axial load for FG microplates with different aspect ratios and various edge supports. Similar results described in figures 5 and 3 can be drawn herein for the effect this parameters. It is seen that frequency response of microplates is different before and after buckling, in a way that microplates with higher aspect ratios have lower natural frequencies in prebuckled configuration and higher frequencies in buckled region.

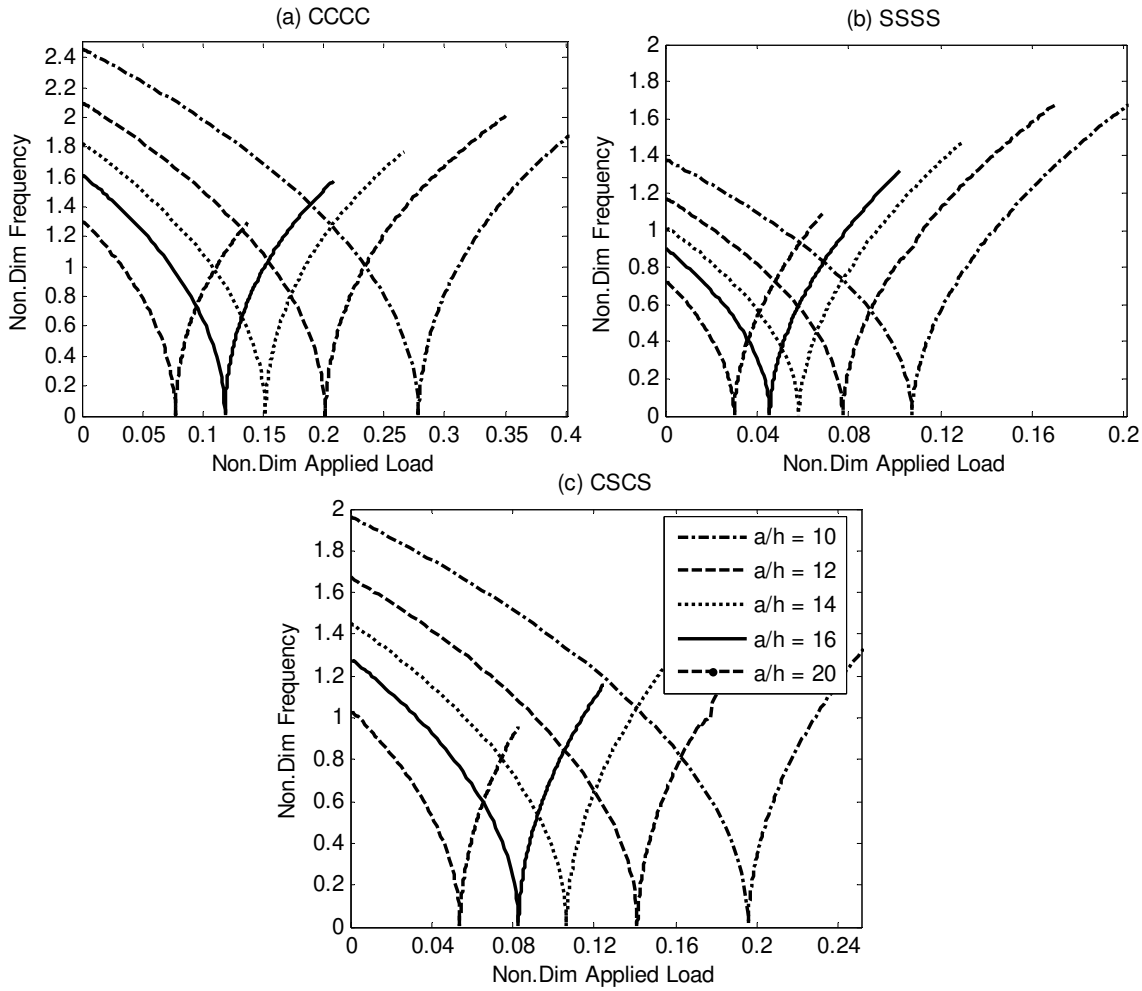

Figure 7: Non-dimensional fundamental natural frequency of the FG microplate around the undeflected and the first buckled configurations versus non-dimensional applied load for different aspect ratios $\left(n = 0.5, h/l = 2,\ b/a = 1\right)$

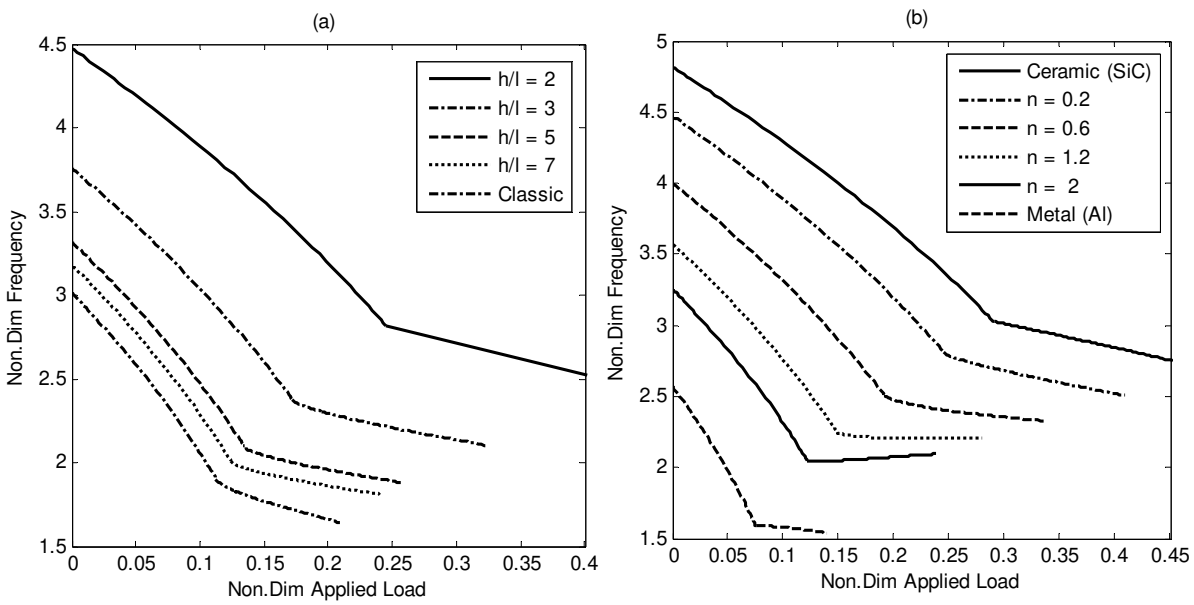

Figure 8: Non-dimensional second frequency of the FG microplate around the undeflected and the first buckledconfigurations versus non-dimensional applied load for different (a) non-dimensional length scale parameters $\left(n = 0.2, a/h = 12,\ b/a = 1\right)$, (b) material gradient indices $\left(h/l = 2,\ a/h = 12,\ b/a = 1\right)$

The effects of non-dimensional length scale parameter and material gradient index on the second frequency of clamped microplates are shown in figure 8. The results show that in an unbuckled equilibrium configuration, the frequencies decease with the increase in the axial applied load. As said before, the first frequency approaches zero at the critical buckling load. But, the higher frequencies go to a minimum value. For the plate in a buckled state, the frequency response of microplate has different behavior corresponding to each vibration modes.

5 CONCLUSION

In the current work, the free vibration behavior of post-buckled functionally graded (FG) Mindlin rectangular microplates was investigated based on the MCST. By using Hamilton's principle, the nonlinear governing equations and associated boundary conditions of FG rectangular microplates in the postbuckling domain were derived. After that, the governing equations and associated boundary conditions were discretized and solved using the GDQ method and the pseudo-arclength continuation technique, respectively. Finally, the influences of effective parameters including length scale parameter, material gradient index, aspect ratio and boundary conditions on the postbuckling path and frequency-response curves of FG rectangular microplates were examined and it was concluded that:

- With the rise of the material gradient index, non-dimensional length scale parameter and aspect ratio, more postbuckled deflections are induced so that the critical applied load declines, indicating lower stability of microplates.

- The necessity of using size-dependent theory to trace the postbuckling path is more felt in microplates with fully clamped edges. Also, this sort of microplates was seen to be more affected by variations of material gradient index and aspect ratio.
- As the applied load increases up to the critical buckling load, the non-dimensional frequency diminishes, while the non-dimensional frequency ascends when the microplate enters the buckled region. Also, it was observed that with the increase of either non-dimensional length scale parameter, material gradient index and aspect ratio, the non-dimensional frequency decreases for microplates in the unbuckled configuration. However, the fundamental frequency grows with the rise of aforementioned parameters in the postbuckling region.

References

Ansari, R., Gholami, R., Darabi, M.A., (2011). Thermal Buckling Analysis of Embedded Single-Walled Carbon Nanotubes with Arbitrary Boundary Conditions Using the Nonlocal Timoshenko Beam Theory. Journal of Thermal Stresses 34: 1271–1281.

Ansari, R., Gholami, R., Darabi M.A., (2012). A Nonlinear Timoshenko Beam Formulation Based on Strain Gradient Theory. Journal of Mechanics of Materials and Structures 7(2): 195-211.

Asghari, M., Ahmadian, M.T., Kahrobaiyan, M.H., Rahaeifard, M., (2010). On the size-dependent behavior of functionally graded micro-beams. Materials & Design 31: 2324–2329.

Asghari, M., Rahaeifard, M., Kahrobaiyan, M.H., Ahmadian, M.T., (2011). The modified couple stress functionally graded Timoshenko beam formulation, Materials & Design 32: 1435–1443.

Chang, T.P., (2013). Nonlinear thermal–mechanical vibration of flow-conveying double-walled carbon nanotubes subjected to random material property. Microfluidics and Nanofluidics 15(2): 219-229.

Claeyssen, J.R., Tsukazan, T., Coppeti, R.D., (2013). Nonlocal effects in modal analysis of forced responses with single carbon nanotubes. Mechanical Systems and Signal Processing 38(2): 299-311.

Eringen, A.C.,(1972). Nonlocal polar elastic continua. International Journal of Engineering Science 10: 1.

Farokhi, H., Ghayesh, M.H., Amabili, M., (2013). Nonlinear dynamics of a geometrically imperfect microbeam based on the modified couple stress theory. International Journal of Engineering Science 68: 11-23.

Fares, M.E., Elmarghany, M.K., Atta D., (2009). An efficient and simple refined theory for bending and vibration of functionally graded plates. Composite Structures 92: 296-305.

Ghayesh, M.H., Amabili, M., Farokhi, H., (2013). Nonlinear forced vibrations of a microbeam based on the strain gradient elasticity theory. International Journal of Engineering Science 63: 52–60.

Hasanyan, D.J., Batra, R.C., Harutyunyan, R.C., (2008). Pull-in instabilities in functionally graded microthermoelectromechanical systems. Journal of Thermal Stresses 31: 1006-1021.

Jomehzadeh, E., Noori, H.R., Saidi, A.R., (2011). The size-dependent vibration analysis of micro-plates based on a modified couple stress theory. Physica E. 43(4): 877–883.

Ke, L.L., Yang, J., Kitipornchai, S., (2010).An Analytical Study on the Nonlinear Vibration of Functionally Graded Beams. Meccanica 45(6): 743-752.

Ke, L.L., Wang, Y.S., (2011). Size effect on dynamic stability of functionally graded microbeams based on a modified couple stress theory. Composite Structures 93: 342–350.

Ke, L.L., Wang, Y.S., Yang, J., Kitipornchai, S., (2011).Nonlinear free vibration of size-dependent functionally graded microbeams. International Journal of Engineering Science 50(1): 256–267.

Ke, L.L., Wang, Y.S., Yang, J., Kitipornchai, S., (2012a). Free vibration of size-dependent Mindlin microplates based on the modified couple stress theory. Journal of Sound and Vibration 331(1): 94-106.

Ke, L.L., Yang, J., Kitipornchai, S., Bradford, M.A., (2012b). Bending, buckling and vibration of size-dependent functionally graded annular microplates. Composite Structures 11(94): 3250-3257.

Keller, H.B.,(1977). Numerical solution of bifurcation and nonlinear eigenvalueproblems, applications of bifurcation theory, Proceedings of the advancedseminar, University of Wisconsin, Madison, Wisconsin, New York:Academic Press: 359–84.

Kovalenko, A.D., (1969). Thermoelasticity, Wolters–Noordhoff Publishing, Gröningen, The Netherlands.

Lam, D.C.C., Yang, F., Chong, A.C.M., Wang, J., Tong, P., (2003). Experiments and theory in strain gradient elasticity. Journal of the Mechanics and Physics of Solids 51: 1477.

Li, S. R., Teng, Z. C., Zhou, Y. H. (2004). Free vibration of heated Euler-Bernoulli beams with thermal postbuckling deformations, Journal of Thermal Stresses 27 (9): 843–856.

Li., S., Batra R. C., Ma L. (2007). Vibration of thermally postbuckled orthotropic circular plate, Journal of Thermal Stresses 30(1): 43–57.

Lü, C.F., Chen W.Q., Lim C.W.,(2009a). Elastic mechanical behavior of nano-scaled FGM films incorporating surface energies, Composites Science and Technology 69: 1124-1130.

Lü, C.F., Lim C.W., Chen W.Q., (2009b). Size-dependent elastic behavior of FGM ultra-thin films based on generalized refined theory, International Journal of Solids and Structures 46: 1176-1185

Mahmud, A.S., Liu, Y., Nam, T.H. (2008). Gradient anneal of functionally graded NiTi. Smart Materials & Structures 17: 015031.

Mindlin, R.D., Tiersten, H.F., (1962). Effects of couple-stresses in linear elasticity. Archive for Rational Mechanics and Analysis 11: 415-448.

Ramezani, S., (2012). A micro scale geometrically non-linear Timoshenko beam model based on strain gradient elasticity theory. International Journal of Non-Linear Mechanics 47(8): 863-873.

Shu, C., (2000). Differential Quadrature and Its Application in Engineering, Springer, London.

Timoshenko, S.P., Goodier J.N., (1970). Theory of Elasticity, third ed. McGraw-Hill, New York.

Toupin, R.A., (1962).Elastic materials with couple-stresses, Archive for Rational Mechanics and Analysis 11: 385.

Tsiatas, G.C., (2009). A new Kirchhoff plate model based on a modified couple stress theory. International Journal of Solids and Structures 46: 2757–2764.

Wang, G.F., Feng, X.Q., (2007). Effects of surface stresses on contact problems at nanoscale. Journal of Applied Physics 101(1): 013510.

Wang, L., (2010), Size-dependent vibration characteristics of fluid-conveying microtubes. Journal of Fluids and Structures,26: 675.

Witvrouw, A., Mehta, A. (2005). The use of functionally graded poly-SiGe layers for MEMS applications. Materials Science Forum 492-493: 255-260.

Yang, F., Chong A.C.M., Lam D.C.C., Tong P., (2002). Couple stress based strain gradient theory for elasticity. International Journal of Solids and Structures 39: 2731-2743.

Yin, L., Xia, W., Wang, L., Qian, Q., (2010). Vibration analysis of micro scale plates based on modified couple stress theory, Acta Mechanica Solida Sinica 23: 386–393.

Zhang, B., Yuming H., Dabiao L., Zhipeng G., Lei S., (2013). A non-classical Mindlin plate finite element based on a modified couple stress theory, European Journal of Mechanics A/Solids 42: 63-80.

Appendix A

The components of stiffness matrix $\mathbf{K}$ are

$$\mathbf{K}_{11} = a_{11}\left(\mathbf{I}_y \otimes \mathbf{D}_x^{(2)}\right) + a_{55}\kappa^2\left(\mathbf{D}_y^{(2)} \otimes \mathbf{I}_x\right) - a_{55}\beta\kappa^4\left(\mathbf{D}_y^{(4)} \otimes \mathbf{I}_x\right) - a_{55}\beta\kappa^2\left(\mathbf{D}_y^{(2)} \otimes \mathbf{D}_x^{(2)}\right),$$

$$\mathbf{K}_{12} = \mathbf{K}_{21} = \kappa\left(a_{12} + a_{55}\right)\left(\mathbf{D}_y^{(1)} \otimes \mathbf{D}_x^{(1)}\right) + a_{55}\beta\kappa\left(\mathbf{D}_y^{(1)} \otimes \mathbf{D}_x^{(3)}\right) + a_{55}\beta\kappa^3\left(\mathbf{D}_y^{(3)} \otimes \mathbf{D}_x^{(1)}\right),$$

$$\mathbf{K}_{13} = \mathbf{K}_{23} = \mathbf{K}_{31} = \mathbf{K}_{32} = \mathbf{0},$$

$$\mathbf{K}_{14} = \mathbf{K}_{41} = -b_{11}\left(\mathbf{I}_y \otimes \mathbf{D}_x^{(2)}\right) - b_{55}\kappa^2\left(\mathbf{D}_y^{(2)} \otimes \mathbf{I}_x\right) + b_{55}\beta\kappa^4\left(\mathbf{D}_y^{(4)} \otimes \mathbf{I}_x\right) + b_{55}\beta\kappa^2\left(\mathbf{D}_y^{(2)} \otimes \mathbf{D}_x^{(2)}\right),$$

$$\mathbf{K}_{15} = \mathbf{K}_{51} = -\kappa\left(b_{12} + b_{55}\right)\left(\mathbf{D}_y^{(1)} \otimes \mathbf{D}_x^{(1)}\right) - b_{55}\beta\kappa\left(\mathbf{D}_y^{(1)} \otimes \mathbf{D}_x^{(3)}\right) - b_{55}\beta\kappa^3\left(\mathbf{D}_y^{(3)} \otimes \mathbf{D}_x^{(1)}\right),$$

$$\mathbf{K}_{22} = \kappa^2 a_{11}\left(\mathbf{D}_y^{(2)} \otimes \mathbf{I}_x\right) + a_{55}\left(\mathbf{I}_y \otimes \mathbf{D}_x^{(2)}\right) - a_{55}\beta\left(\mathbf{I}_y \otimes \mathbf{D}_x^{(4)}\right) - a_{55}\beta\kappa^2\left(\mathbf{D}_y^{(2)} \otimes \mathbf{D}_x^{(2)}\right),$$

$$\mathbf{K}_{24} = \mathbf{K}_{42} = -\kappa\left(b_{12} + b_{55}\right)\left(\mathbf{D}_y^{(1)} \otimes \mathbf{D}_x^{(1)}\right) - b_{55}\beta\kappa\left(\mathbf{D}_y^{(1)} \otimes \mathbf{D}_x^{(3)}\right) - b_{55}\beta\kappa^3\left(\mathbf{D}_y^{(3)} \otimes \mathbf{D}_x^{(1)}\right),$$

$$\mathbf{K}_{25} = \mathbf{K}_{52} = -\kappa^2 b_{11}\left(\mathbf{D}_y^{(2)} \otimes \mathbf{I}_x\right) - b_{55}\left(\mathbf{I}_y \otimes \mathbf{D}_x^{(2)}\right) + b_{55}\beta\left(\mathbf{I}_y \otimes \mathbf{D}_x^{(4)}\right) + b_{55}\beta\kappa^2\left(\mathbf{D}_y^{(2)} \otimes \mathbf{D}_x^{(2)}\right),$$

$$\mathbf{K}_{33} = k_s a_{55}\left[\left(\mathbf{I}_y \otimes \mathbf{D}_x^{(2)}\right) + \kappa^2\left(\mathbf{D}_y^{(2)} \otimes \mathbf{I}_x\right)\right] - a_{55}\beta\left[\left(\mathbf{I}_y \otimes \mathbf{D}_x^{(4)}\right) + 2\kappa^2\left(\mathbf{D}_y^{(2)} \otimes \mathbf{D}_x^{(2)}\right) + \kappa^4\left(\mathbf{D}_y^{(4)} \otimes \mathbf{I}_x\right)\right],$$

$$\mathbf{K}_{34} = -\mathbf{K}_{43} = -k_s a_{55}\eta_1\left(\mathbf{I}_y \otimes \mathbf{D}_x^{(1)}\right) - a_{55}\beta\eta_1\left[\left(\mathbf{I}_y \otimes \mathbf{D}_x^{(3)}\right) + \kappa^2\left(\mathbf{D}_y^{(2)} \otimes \mathbf{D}_x^{(1)}\right)\right],$$

$$\mathbf{K}_{35} = -\mathbf{K}_{53} = -k_s a_{55}\eta_1\kappa\left(\mathbf{D}_y^{(1)} \otimes \mathbf{I}_x\right) - a_{55}\beta\eta_1\left[\kappa\left(\mathbf{D}_y^{(1)} \otimes \mathbf{D}_x^{(2)}\right) + \kappa^3\left(\mathbf{D}_y^{(3)} \otimes \mathbf{I}_x\right)\right],$$

$$\mathbf{K}_{44} = d_{11}\left(\mathbf{I}_y \otimes \mathbf{D}_x^{(2)}\right) + \kappa^2 d_{55}\left(\mathbf{D}_y^{(2)} \otimes \mathbf{I}_x\right) - k_s a_{55}\eta_1^2\left(\mathbf{I}_y \otimes \mathbf{I}_x\right)$$
$$- d_{55}\beta\kappa^2\left[\left(\mathbf{D}_y^{(2)} \otimes \mathbf{D}_x^{(2)}\right) + \kappa^2\left(\mathbf{D}_y^{(4)} \otimes \mathbf{I}_x\right)\right] + a_{55}\ell^2\left[\frac{1}{4}\left(\mathbf{I}_y \otimes \mathbf{D}_x^{(2)}\right) + \kappa^2\left(\mathbf{D}_y^{(2)} \otimes \mathbf{I}_x\right)\right],$$

$$\mathbf{K}_{45} = \mathbf{K}_{54} = \left[\kappa\left(d_{55} + d_{12}\right) - \frac{3a_{55}\ell^2\kappa}{4}\right]\left(\mathbf{D}_y^{(1)} \otimes \mathbf{D}_x^{(1)}\right) + d_{55}\beta\kappa\left(\mathbf{D}_y^{(1)} \otimes \mathbf{D}_x^{(3)}\right) + d_{55}\beta\kappa^3\left(\mathbf{D}_y^{(3)} \otimes \mathbf{D}_x^{(1)}\right),$$

$$\mathbf{K}_{55} = \kappa^2 d_{11}\left(\mathbf{D}_y^{(2)} \otimes \mathbf{I}_x\right) + d_{55}\left(\mathbf{I}_y \otimes \mathbf{D}_x^{(2)}\right) - k_s a_{55}\eta_1^2\left(\mathbf{I}_y \otimes \mathbf{I}_x\right)$$
$$- d_{55}\beta\left[\kappa^2\left(\mathbf{D}_y^{(2)} \otimes \mathbf{D}_x^{(2)}\right) + \left(\mathbf{I}_y \otimes \mathbf{D}_x^{(4)}\right)\right] + a_{55}\ell^2\left[\left(\mathbf{I}_y \otimes \mathbf{D}_x^{(2)}\right) + \frac{\kappa^2}{4}\left(\mathbf{D}_y^{(2)} \otimes \mathbf{I}_x\right)\right],$$

Appendix B

$\mathbf{R}_1$, $\mathbf{R}_2, \mathbf{R}_3$, $\mathbf{R}_4$ and $\mathbf{R}_5$ including the nonlinear terms are

$$\mathbf{R}_1 = \frac{1}{\eta_1}\left(a_{11}\left(\left(\mathbf{I}_y \otimes \mathbf{D}_x^{(1)}\right)\bar{\mathbf{w}}_s\right)\circ\left(\left(\mathbf{I}_y \otimes \mathbf{D}_x^{(2)}\right)\bar{\mathbf{w}}_s\right) + \left(a_{12}+a_{55}\right)\kappa^2\left(\left(\mathbf{D}_y^{(1)} \otimes \mathbf{I}_x\right)\bar{\mathbf{w}}_s\right)\circ\left(\left(\mathbf{D}_y^{(1)} \otimes \mathbf{D}_x^{(1)}\right)\bar{\mathbf{w}}_s\right)\right)$$
$$+ \frac{a_{55}\kappa^2}{\eta_1}\left(\left(\mathbf{I}_y \otimes \mathbf{D}_x^{(1)}\right)\bar{\mathbf{w}}_s\right)\circ\left(\left(\mathbf{D}_y^{(2)} \otimes \mathbf{I}_x\right)\bar{\mathbf{w}}_s\right),$$

$$\mathbf{R}_3 = \frac{a_{11}}{\eta_1}\left(\left(\left(\mathbf{I}_y \otimes \mathbf{D}_x^{(1)}\right)\bar{\mathbf{u}}_s\right) + \frac{1}{2\eta_1}\left(\left(\mathbf{I}_y \otimes \mathbf{D}_x^{(1)}\right)\bar{\mathbf{w}}_s\right)\circ\left(\left(\mathbf{I}_y \otimes \mathbf{D}_x^{(1)}\right)\bar{\mathbf{w}}_s\right)\right)\circ\left(\left(\mathbf{I}_y \otimes \mathbf{D}_x^{(2)}\right)\bar{\mathbf{w}}_s\right)$$
$$+ \frac{a_{12}\kappa}{\eta_1}\left(\left(\left(\mathbf{D}_y^{(1)} \otimes \mathbf{I}_x\right)\bar{\mathbf{v}}_s\right) + \frac{1}{2\eta_2}\left(\left(\mathbf{D}_y^{(1)} \otimes \mathbf{I}_x\right)\bar{\mathbf{w}}_s\right)\circ\left(\left(\mathbf{D}_y^{(1)} \otimes \mathbf{I}_x\right)\bar{\mathbf{w}}_s\right)\right)\circ\left(\left(\mathbf{I}_y \otimes \mathbf{D}_x^{(2)}\right)\bar{\mathbf{w}}_s\right)$$
$$- \frac{b_{12}\kappa}{\eta_1}\left(\left(\mathbf{D}_y^{(1)} \otimes \mathbf{I}_x\right)\bar{\psi}_{y_s}\right)\circ\left(\left(\mathbf{I}_y \otimes \mathbf{D}_x^{(2)}\right)\bar{\mathbf{w}}_s\right) - \frac{b_{11}}{\eta_1}\left(\left(\mathbf{I}_y \otimes \mathbf{D}_x^{(1)}\right)\bar{\psi}_{x_s}\right)\circ\left(\left(\mathbf{I}_y \otimes \mathbf{D}_x^{(2)}\right)\bar{\mathbf{w}}_s\right)$$
$$+ \frac{a_{11}\kappa^3}{\eta_1}\left(\left(\left(\mathbf{D}_y^{(1)} \otimes \mathbf{I}_x\right)\bar{\mathbf{v}}_s\right) + \frac{1}{2\eta_2}\left(\left(\mathbf{D}_y^{(1)} \otimes \mathbf{I}_x\right)\bar{\mathbf{w}}_s\right)\circ\left(\left(\mathbf{D}_y^{(1)} \otimes \mathbf{I}_x\right)\bar{\mathbf{w}}_s\right)\right)\circ\left(\left(\mathbf{D}_y^{(2)} \otimes \mathbf{I}_x\right)\bar{\mathbf{w}}_s\right)$$
$$+ \frac{a_{12}\kappa^2}{\eta_1}\left(\left(\left(\mathbf{I}_y \otimes \mathbf{D}_x^{(1)}\right)\bar{\mathbf{u}}_s\right) + \frac{1}{2\eta_1}\left(\left(\mathbf{I}_y \otimes \mathbf{D}_x^{(1)}\right)\bar{\mathbf{w}}_s\right)\circ\left(\left(\mathbf{I}_y \otimes \mathbf{D}_x^{(1)}\right)\bar{\mathbf{w}}_s\right)\right)\circ\left(\left(\mathbf{D}_y^{(2)} \otimes \mathbf{I}_x\right)\bar{\mathbf{w}}_s\right)$$
$$- \frac{b_{11}\kappa^3}{\eta_1}\left(\left(\mathbf{D}_y^{(1)} \otimes \mathbf{I}_x\right)\bar{\psi}_{y_s}\right)\circ\left(\left(\mathbf{D}_y^{(2)} \otimes \mathbf{I}_x\right)\bar{\mathbf{w}}_s\right) - \frac{b_{12}\kappa^2}{\eta_1}\left(\left(\mathbf{I}_y \otimes \mathbf{D}_x^{(1)}\right)\bar{\psi}_{x_s}\right)\circ\left(\left(\mathbf{D}_y^{(2)} \otimes \mathbf{I}_x\right)\bar{\mathbf{w}}_s\right)$$
$$+ \frac{2\kappa a_{55}}{\eta_1}\left(\kappa\left(\left(\mathbf{D}_y^{(1)} \otimes \mathbf{I}_x\right)\bar{\mathbf{u}}_s\right) + \left(\left(\mathbf{I}_y \otimes \mathbf{D}_x^{(1)}\right)\bar{\mathbf{v}}_s\right) + \frac{\kappa}{\eta_1}\left(\left(\mathbf{D}_y^{(1)} \otimes \mathbf{I}_x\right)\bar{\mathbf{w}}_s\right)\circ\left(\left(\mathbf{D}_y^{(1)} \otimes \mathbf{I}_x\right)\bar{\mathbf{w}}_s\right)\right)\circ\left(\left(\mathbf{D}_y^{(1)} \otimes \mathbf{D}_x^{(1)}\right)\bar{\mathbf{w}}_s\right)$$
$$- \frac{2\kappa b_{55}}{\eta_1}\left(\kappa\left(\left(\mathbf{D}_y^{(1)} \otimes \mathbf{I}_x\right)\bar{\psi}_{x_s}\right) + \left(\left(\mathbf{I}_y \otimes \mathbf{D}_x^{(1)}\right)\bar{\psi}_{y_s}\right)\right)\circ\left(\left(\mathbf{D}_y^{(1)} \otimes \mathbf{D}_x^{(1)}\right)\bar{\mathbf{w}}_s\right)$$
$$+ \frac{a_{11}}{\eta_1}\left(\left(\left(\mathbf{I}_y \otimes \mathbf{D}_x^{(2)}\right)\bar{\mathbf{u}}_s\right) + \frac{1}{\eta_1}\left(\left(\mathbf{I}_y \otimes \mathbf{D}_x^{(1)}\right)\bar{\mathbf{w}}_s\right)\circ\left(\left(\mathbf{I}_y \otimes \mathbf{D}_x^{(2)}\right)\bar{\mathbf{w}}_s\right)\right)\circ\left(\left(\mathbf{I}_y \otimes \mathbf{D}_x^{(1)}\right)\bar{\mathbf{w}}_s\right)$$
$$+ \frac{a_{12}\kappa}{\eta_1}\left(\left(\left(\mathbf{D}_y^{(1)} \otimes \mathbf{D}_x^{(1)}\right)\bar{\mathbf{v}}_s\right) + \frac{1}{\eta_2}\left(\left(\mathrm{D}_y^{(1)} \otimes \mathbf{I}_x\right)\bar{\mathbf{w}}_s\right)\circ\left(\left(\mathbf{D}_y^{(1)} \otimes \mathbf{D}_x^{(1)}\right)\bar{\mathbf{w}}_s\right)\right)\circ\left(\left(\mathbf{I}_y \otimes \mathbf{D}_x^{(1)}\right)\bar{\mathbf{w}}_s\right)$$
$$- \frac{1}{\eta_1}\left(b_{11}\left(\left(\mathbf{I}_y \otimes \mathbf{D}_x^{(2)}\right)\bar{\psi}_{x_s}\right) + b_{12}\kappa\left(\left(\mathbf{D}_y^{(1)} \otimes \mathbf{D}_x^{(1)}\right)\bar{\psi}_{y_s}\right)\right)\circ\left(\left(\mathbf{I}_y \otimes \mathbf{D}_x^{(1)}\right)\bar{\mathbf{w}}_s\right)$$

$$\mathbf{R}_2 = \frac{1}{\eta_1}\left(a_{11}\kappa^3\left(\left(\mathbf{D}_y^{(1)} \otimes \mathbf{I}_x\right)\bar{\mathbf{w}}_s\right)\circ\left(\left(\mathbf{D}_y^{(2)} \otimes \mathbf{I}_x\right)\bar{\mathbf{w}}_s\right) + \left(a_{12}+a_{55}\right)\kappa\left(\left(\mathbf{I}_y \otimes \mathbf{D}_x^{(1)}\right)\bar{\mathbf{w}}_s\right)\circ\left(\left(\mathbf{D}_y^{(1)} \otimes \mathbf{D}_x^{(1)}\right)\bar{\mathbf{w}}_s\right)\right)$$
$$+ \frac{a_{55}\kappa}{\eta_1}\left(\left(\mathbf{I}_y \otimes \mathbf{D}_x^{(2)}\right)\bar{\mathbf{w}}_s\right)\circ\left(\left(\mathbf{D}_y^{(1)} \otimes \mathbf{I}_x\right)\bar{\mathbf{w}}_s\right),$$

$$+\frac{a_{55}\kappa}{\eta_1}\left(\kappa\left(\left(\mathbf{D}_y^{(1)}\otimes\mathbf{D}_x^{(1)}\right)\bar{\mathbf{u}}_s\right)+\left(\left(\mathbf{I}_y\otimes \mathrm{D}_x^{(2)}\right)\bar{\mathbf{v}}_s\right)\right)\circ\left(\left(\mathbf{D}_y^{(1)}\otimes\mathbf{I}_x\right)\bar{\mathbf{w}}_s\right)$$

$$+\frac{\kappa a_{55}}{\eta_1}\left(\frac{\kappa}{\eta_1}\left(\left(\mathbf{I}_y\otimes \mathrm{D}_x^{(2)}\right)\bar{\mathbf{w}}_s\right)\circ\left(\left(\mathbf{D}_y^{(1)}\otimes\mathbf{I}_x\right)\bar{\mathbf{w}}_s\right)+\frac{\kappa}{\eta_1}\left(\left(\mathbf{I}_y\otimes\mathbf{D}_x^{(1)}\right)\bar{\mathbf{w}}_s\right)\circ\left(\left(\mathbf{D}_y^{(1)}\otimes\mathbf{D}_x^{(1)}\right)\bar{\mathbf{w}}_s\right)\right)\circ\left(\left(\mathbf{D}_y^{(1)}\otimes\mathbf{I}_x\right)\bar{\mathbf{w}}_s\right)$$

$$-\frac{b_{55}\kappa}{\eta_1}\left(\left(\kappa\left(\left(\mathbf{D}_y^{(1)}\otimes\mathbf{D}_x^{(1)}\right)\bar{\boldsymbol{\psi}}_{\mathrm{x}_s}\right)+\left(\left(\mathbf{I}_y\otimes\mathbf{D}_{\mathrm{x}}^{(2)}\right)\bar{\boldsymbol{\psi}}_{\mathrm{y}_s}\right)\right)\right)\circ\left(\left(\mathbf{D}_y^{(1)}\otimes\mathbf{I}_x\right)\bar{\mathbf{w}}_s\right)$$

$$+\frac{a_{55}\kappa}{\eta_1}\left(\kappa\left(\left(\mathbf{D}_y^{(2)}\otimes\mathbf{I}_x\right)\bar{\mathbf{u}}_s\right)+\left(\left(\mathbf{D}_y^{(1)}\otimes\mathbf{D}_x^{(1)}\right)\bar{\mathbf{v}}_s\right)\right)\circ\left(\left(\mathbf{I}_y\otimes\mathbf{D}_x^{(1)}\right)\bar{\mathbf{w}}_s\right)$$

$$+\frac{a_{55}\kappa^2}{\eta_1^2}\left(\left(\left(\mathbf{D}_y^{(1)}\otimes\mathbf{D}_x^{(1)}\right)\bar{\mathbf{w}}_s\right)\circ\left(\left(\mathbf{D}_y^{(1)}\otimes\mathbf{I}_x\right)\bar{\mathbf{w}}_s\right)+\left(\left(\mathbf{I}_y\otimes\mathbf{D}_x^{(1)}\right)\bar{\mathbf{w}}_s\right)\circ\left(\left(\mathbf{D}_y^{(2)}\otimes\mathbf{I}_x\right)\bar{\mathbf{w}}_s\right)\right)\circ\left(\left(\mathbf{I}_y\otimes\mathbf{D}_x^{(1)}\right)\bar{\mathbf{w}}_s\right)$$

$$-\frac{b_{55}\kappa}{\eta_1}\left(\left(\kappa\left(\left(\mathbf{D}_y^{(2)}\otimes\mathbf{I}_x\right)\bar{\boldsymbol{\psi}}_{\mathrm{x}_s}\right)+\left(\left(\mathbf{D}_y^{(1)}\otimes\mathbf{D}_x^{(1)}\right)\bar{\boldsymbol{\psi}}_{\mathrm{y}_s}\right)\right)\right)\circ\left(\left(\mathbf{I}_y\otimes\mathbf{D}_x^{(1)}\right)\bar{\mathbf{w}}_s\right)$$

$$+\frac{\kappa^3 a_{11}}{\eta_1}\left(\left(\left(\mathbf{D}_y^{(2)}\otimes\mathbf{I}_x\right)\bar{\mathbf{v}}_s\right)+\frac{1}{\eta_2}\left(\left(\mathbf{D}_y^{(1)}\otimes\mathbf{I}_x\right)\bar{\mathbf{v}}_s\right)\circ\left(\left(\mathbf{D}_y^{(2)}\otimes\mathbf{I}_x\right)\bar{\mathbf{v}}_s\right)\right)\circ\left(\left(\mathbf{D}_y^{(1)}\otimes\mathbf{I}_x\right)\bar{\mathbf{w}}_s\right)$$

$$+\frac{\kappa^2 a_{12}}{\eta_1}\left(\left(\left(\mathbf{D}_y^{(1)}\otimes\mathbf{D}_x^{(1)}\right)\bar{\mathbf{u}}_s\right)+\frac{1}{\eta_1}\left(\left(\mathbf{I}_y\otimes\mathbf{D}_x^{(1)}\right)\bar{\mathbf{w}}_s\right)\circ\left(\left(\mathbf{D}_y^{(1)}\otimes\mathbf{D}_x^{(1)}\right)\bar{\mathbf{w}}_s\right)\right)\circ\left(\left(\mathbf{D}_y^{(1)}\otimes\mathbf{I}_x\right)\bar{\mathbf{w}}_s\right)$$

$$+\frac{\kappa^2}{\eta_1}\left(-b_{11}\kappa\left(\left(\mathbf{D}_y^{(2)}\otimes\mathbf{I}_x\right)\bar{\boldsymbol{\psi}}_{\mathrm{y}_s}\right)-b_{12}\left(\left(\mathbf{D}_y^{(1)}\otimes\mathbf{D}_x^{(1)}\right)\bar{\boldsymbol{\psi}}_{\mathrm{x}_s}\right)\right)\circ\left(\left(\mathbf{D}_y^{(1)}\otimes\mathbf{I}_x\right)\bar{\mathbf{w}}_s\right),$$

$$\mathbf{R}_4=\frac{b_{11}}{\eta_1}\left(\left(\mathbf{I}_y\otimes\mathbf{D}_x^{(1)}\right)\bar{\mathbf{w}}_s\right)\circ\left(\left(\mathbf{I}_y\otimes\mathbf{D}_x^{(2)}\right)\bar{\mathbf{w}}_s\right)+\frac{b_{55}\kappa^2}{\eta_1}\left(\left(\mathbf{I}_y\otimes\mathbf{D}_x^{(1)}\right)\bar{\mathbf{w}}_s\right)\circ\left(\left(\mathbf{D}_y^{(2)}\otimes\mathbf{I}_x\right)\bar{\mathbf{w}}_s\right)$$
$$+\frac{\left(b_{12}+b_{55}\right)\kappa^2}{\eta_1}\left(\left(\mathbf{D}_y^{(1)}\otimes\mathbf{I}_x\right)\bar{\mathbf{w}}_s\right)\circ\left(\left(\mathbf{D}_y^{(1)}\otimes\mathbf{D}_x^{(1)}\right)\bar{\mathbf{w}}_s\right)\circ\left(\left(\mathbf{D}_y^{(2)}\otimes\mathbf{I}_x\right)\bar{\mathbf{w}}_s\right),$$

$$\mathbf{R}_5=\frac{b_{11}\kappa^3}{\eta_1}\left(\left(\mathbf{D}_y^{(1)}\otimes\mathbf{I}_x\right)\bar{\mathbf{w}}_s\right)\circ\left(\left(\mathbf{D}_y^{(2)}\otimes\mathbf{I}_x\right)\bar{\mathbf{w}}_s\right)+\frac{b_{55}\kappa}{\eta_1}\left(\left(\mathbf{I}_y\otimes\mathbf{D}_x^{(2)}\right)\bar{\mathbf{w}}_s\right)\circ\left(\left(\mathbf{D}_y^{(1)}\otimes\mathbf{I}_x\right)\bar{\mathbf{w}}_s\right)$$
$$+\frac{\left(b_{12}+b_{55}\right)\kappa}{\eta_1}\left(\left(\mathbf{I}_y\otimes\mathbf{D}_x^{(1)}\right)\bar{\mathbf{w}}_s\right)\circ\left(\left(\mathbf{D}_y^{(1)}\otimes\mathbf{D}_x^{(1)}\right)\bar{\mathbf{w}}_s\right).$$

The boundary conditions are similarly discretized.